

ARCHAEOLOGICAL ANALYSIS OF MORTARS FROM THE ROMAN VILLA RUSTICA AT ŠKOLARICE (SLOVENIA)

Anthony J. BARAGONA

University of Applied Arts Vienna, Institute of Conservation, Salzgies 14/1, 1013 Vienna, Austria
e-mail: tonybaragona@gmail.com

Katharina ZANIER

University of Ljubljana, Faculty of Arts, Department of Archaeology, Zavetiška 5, 1000 Ljubljana, Slovenia
e-mail: katharina.zanier@ff.uni-lj.si

Dita FRANKOVÁ

Czech Academy of Sciences, Institute of Theoretical and Applied Mechanics, Prosecká 809/76, Prague 9-Prosek, Czech Republic
e-mail: frankeova@itam.cas.cz

Marta ANGHELONE

University of Applied Arts Vienna, Institute of Conservation, Salzgies 14/1, 1013 Vienna, Austria
e-mail: marta.anghelone@uni-ak.ac.at

Johannes WEBER

University of Applied Arts Vienna, Institute of Conservation, Salzgies 14/1, 1013 Vienna, Austria
e-mail: johannes.weber@uni-ak.ac.at

ABSTRACT

This paper reports the results of the analysis of mortars used in the Roman villa at Školarice, Slovenia. The samples were analysed by optical microscopy (OM), scanning electron microscopy coupled with energy-dispersive X-ray spectroscopy (SEM-EDX) and Fourier-transform infrared spectroscopy imaging (FTIR-i). The hydraulicity was determined for the ceramic-lime (“cocciopesto”) mortars by chemical dissolution methods, thermo-gravimetric analysis – differential scanning calorimetry (TGA-DSC) as well as binder area analysis by EDX and FTIR-i on the corresponding thin sections. The results helped in the interpretation of the site especially in relation to the extent of use of crushed ceramic as a pozzolanic or waterproofing material.

Keywords: Roman villa, Školarice, historical mortar, FTIR-imaging, hydraulicity index

ANALISI ARCHEOMETRICA DI MALTE DALLA VILLA RUSTICA ROMANA DI ŠKOLARICE (SLOVENIA)

SINTESI

In questo contributo riportiamo i risultati dell'analisi di malte della villa romana di Školarice in Slovenia. I campioni sono stati analizzati mediante microscopia ottica (OM), microscopia elettronica a scansione accoppiata con spettroscopia a raggi X in dispersione di energia (SEM-EDX) e spettroscopia a infrarossi in trasformata di Fourier (FTIR-i). L'idraulicità è stata determinata per le malte a base di calce e cocciopesto con metodi di dissoluzione chimica, analisi termogravimetrica – calorimetria differenziale a scansione (TGA-DSC) e analisi dell'area del legante mediante EDX e FTIR-i sulle sezioni sottili corrispondenti. I risultati hanno fornito importanti spunti per l'interpretazione del sito, in particolare in relazione all'entità dell'uso di cocciopesto come materiale pozzolanico o impermeabilizzante.

Parole chiave: Villa romana, Scoladizzi / Školarice, malte storiche, spettrofotometria in trasformata di Fourier (FTIR-i), indice di idraulicità

INTRODUCTION

Background of the Site

The Roman *villa rustica* at Školarice is located not far from the south-western coast of Slovenia on the very northern edge of the Mediterranean. During the archaeological excavation of the site in 2002, which covered a surface area of 6136 m², several rooms were discovered, mostly consisting of the productive part of the villa but also including a thermal complex. However, the area explored represents only a fraction of the entire ancient villa complex. Due to the site's sloping terrain the complex was built on terraces descending towards the southwest (Figure 1). On the lower, south terrace, a small part of the residential area and baths were discovered, preserved only at the foundation level (Figure 2); unfortunately, large portions of this area were removed during construction work in the 1960s. The upper terrace was built on sloping levels with a large storehouse and rooms used to produce wine, oil and possibly even flour. The remains of a *torcularium* paved with coarse mosaic were found here (Figures 3, 4) as well. Various open areas used as courtyards completed the complex. The villa was erected over an earlier building towards the middle of the 1st century AD, remaining in use until the mid-5th century AD; the development of the site is divided into 6 main phases, partly divided into subphases (Trenz & Novšak, 2004; Novšak & Žerjal, 2008; Sakara Sučević *et al.*, 2015; Gutman *et al.*, 2016; Žerjal & Novšak, 2020). In ancient times the villa was placed in the territory of the colony of *Tergeste*, within the *Regio X (Venetia et Histria)* of Roman Italy, along the Roman road *Via Flavia* that connected *Tergeste* (Trieste) to *Parentium* (Poreč) and *Pola* (Pula). For immediate proximity to the main route of the *Via Flavia*, as also for planimetric reasons (cf. Ventura, 2001), the villa appears very likely to have also functioned as a *mansio* (Zanier, 2012, 316). The site is also near to the Rižana river and could therefore be tentatively identified as *Aquae Risani*, meaning the 'Baths of Rižana', perhaps shown on the *Tabula Peutingeriana*, as "Quaeri" (symbolized by a road station with baths) (Degrassi, 1939, 68; Bosio, 1991, 232); the later Italian name of the area is "Scoladizzi" (from Italian *scolare*, i. e. 'flow, drain'), transformed into Slovenian as "Školarice" (Žerjal & Novšak, 2020, 9).

Damage to the southern terrace, which is the residential area of the villa, resulted in the extensive loss of floors and wall paintings. As a consequence, only a few high-quality wall painting fragments with more refined decorative motifs, such as those exhibiting stucco decoration, were collected during the archaeological excavation of the thermal area (Zanier, 2012; Zanier, 2020). Similarly decorated stucco cornices are typical of the final Third and especially the Fourth Pompeian Styles of the second half of the 1st century AD (Riemen-

schneider, 1986; Fröhlich, 1995). Across the entire complex plain wall paintings are predominant; they show fairly homogeneous preparations characterized by very simple decorations including yellow, red, burgundy red, green and black panels, sometimes bounded by white stripes, as well as white panels bordered by broad red bands. These patterns reflect the wide spectrum of plain decorations based on chromatic and modular strings of panels of interchanging colours, which were especially in use from the second half of the 1st through the 2nd century AD (Salvadori, 2012).

Previous Relevant Research and Analytical Overview

Paint layer stratigraphy and painting techniques of selected wall painting samples were studied previously by using optical microscopy, with pigments identified via Raman micro-spectroscopy supported by FTIR-i micro-spectroscopy and SEM/EDS (Gutman *et al.*, 2016). Different tonalities of the red paint layers were composed either by a mixture of red ochre (hematite) and yellow ochre (goethite) or by hematite alone. For yellow paint layers, goethite was used, for green celadonite, for black tones carbon black and for white ones, calcite. Paintings were applied in fresco, but details (fillets and similar) were applied in secco. Green and red paint layers are sometimes applied on yellow underpaint, which was probably meant to have positive effects on the luminescence of the colour (Gutman *et al.*, 2016, 201–204). The pigments used and implied technical solutions (mixtures of pigments, double colour layers, combination of fresco and secco techniques) show that skilled artisans were active here (Zanier, 2020).

The primary tool used for this study of the mortars used at Školarice was the employment of a stepwise protocol of microscopic and micro-analytical techniques performed on polished (uncovered) petrographic thin sections of 12 of the 19 mortars provided; the remaining 7 were studied by microscopy of cross sections and chemical analysis, allowing for correlations to be made with the mortars from which thin sections had been produced. The 12 thin sections were studied in sequence by optical microscopy (OM), scanning electron microscopy and energy dispersive x-ray spectroscopy (SEM-EDX) and Fourier-transform infra-red spectroscopy imaging (FTIR-i). While these first two techniques are commonly used on thin sections, FTIR-i is less, so this research was performed in an innovative manner. Polished petrographic thin sections preserve the micro-structural features of a mortar, such as the shape and quantity of porosity, relics of the binder source and a wide variety of reaction and alteration products, and importantly how they relate to one another – information that is lost when a mortar is analysed by chemical or thermal dissolution techniques (Elsen, 2006). Studying these features by image-based means is the key to fully understanding both the materials and methods of the responsible artisan, as well

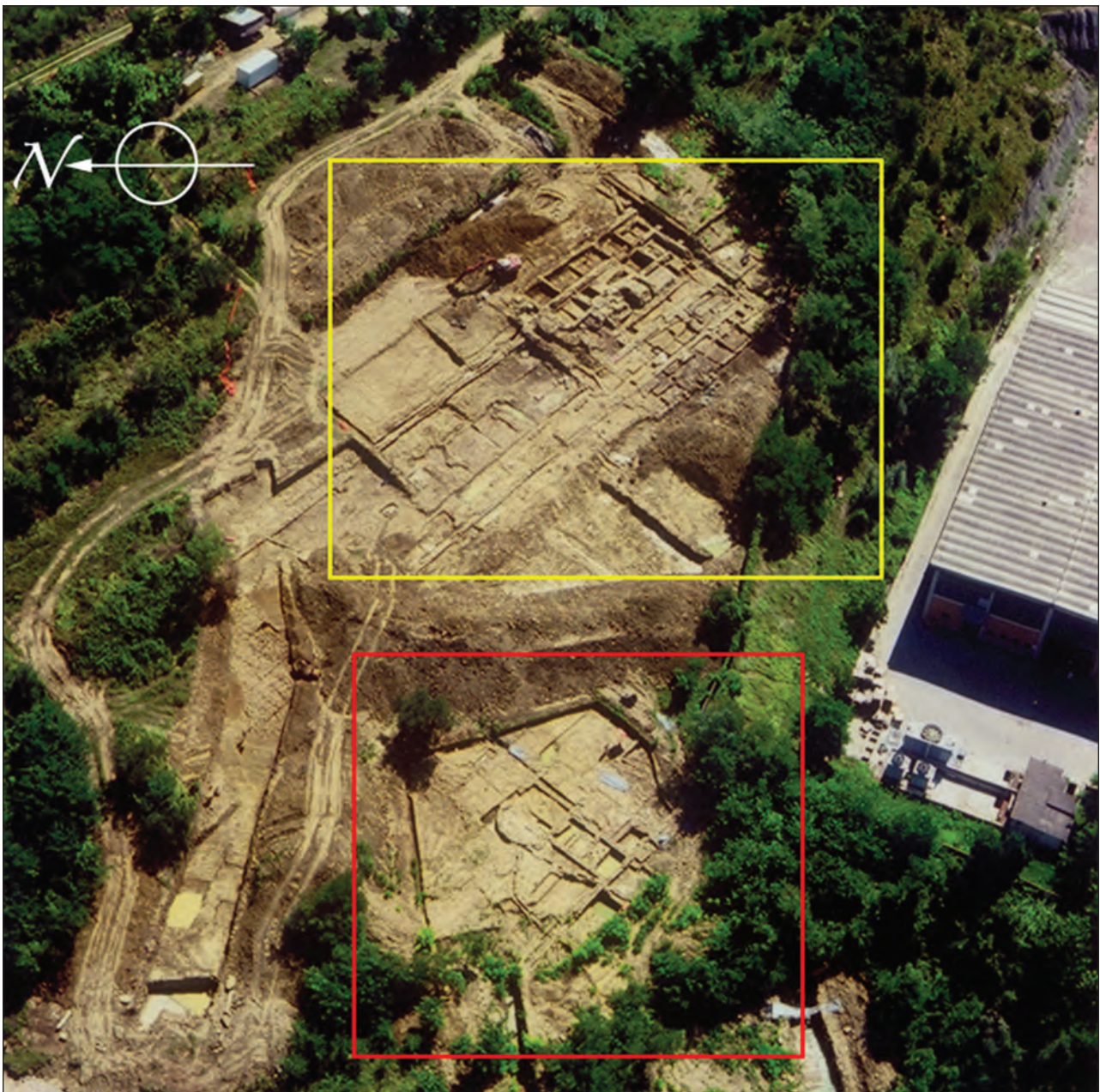


Figure 1: Školarice: Roman villa, 2002 excavations (by J. Jeraša, archive Arhej d. o. o.). Red box – thermal area, yellow box – production area.

as how a mortar has changed over time (Weber *et al.*, 2009; Weber & Baragona 2021; Baragona, 2021).

A portion of the mortars described herein utilized a reaction between reactive ceramic aggregates (pozzolans) and calcium hydroxide to form a hydraulic binder through the pozzolanic reaction to produce calcium-alumina-silicate-hydrate (“C-A-S-H”) (Mehta, 1987; Massazza, 2001; Snellings *et al.*, 2012). In the Roman era, these were often used in areas of high humidity or in direct contact with water, such as flooring or the

walls of a bath or cistern (Adam, 1994; Miriello *et al.*, 2010). These mortars were given special attention, as they are particularly helpful in determining/ confirming the use of a structure. One means of quantifying a mortar’s binder hydraulicity is its hydraulicity index (HI), derived from the formula: $\text{SiO}_2 + \text{Al}_2\text{O}_3 / \text{CaO}$ detected in a binder, per Boynton’s second equation (Boynton, 1980; Elsen *et al.*, 2010).

In our study, this was determined for 5 representative samples by 4 different methods: EDX and FTIR-i on the

binder areas of polished thin sections, as well as both chemical dissolution and thermogravimetric analysis (TGA) of a different portion of the same samples. The method using FTIR-i, described further below is a novel technique developed during the first author's dissertation work at the University of Applied Arts, Vienna. Therefore, determining the HI by these 4 different methods on the mortar of Školarice provided an opportunity to prove the efficacy of the novel technique, in that it gave comparable results to the other 3 (see Section 3.5 and Table 3) and this probably represents the most important contribution of this paper. These results were then correlated with similar samples (that were, in the interest of economy of time and resources, not prepared as polished thin section) from the site to understand where and why these types of mortars were used. The paper reveals the use of the best mortar for each condition and structural need by the builders of the villa at Školarice throughout different structures and building phases. In doing so, they achieved the high-quality standard of construction found throughout the Roman Empire.

MATERIALS AND METHODS

Sample Provenance

For the purpose of this study, 19 samples from different locations and phases of the villa were analysed: 13 from the thermal area on the lower terrace and 6 from the productive area situated in the north-eastern, higher part of the complex. Samples were selected with the aim of including potentially pozzolanic mortars, i.e. with visually recognizable ceramic or volcanic aggregates and/or a pinkish binder hue.

Two analysed fragments of painted wall plaster (samples Ško-101.1 and Ško-101.2) were found within

a secondary context of a recent rubble layer extending over the lower terrace of the thermal area. They likely pertained to its decoration, but it is not possible to define the specific room of provenance and phase. One mortar sample (Ško-310) was sampled in room 4 of the thermal area, but in a wall foundation (adjacent to the western wall of room 4) pertaining to an earlier building that predates the construction of the villa. The thermal area has two apsidated rooms (3 and 4) recognizable as *frigidarium* and *calidarium* (Figure 2). In between, there were rooms 5 and 6. The *praeefurnia* were identified in room 10. To the west of the baths, there is an open courtyard (the external western courtyard), which was originally paved with irregular stone elements (with sizes from 10 x 9 x 3 to 21 x 20 x 7 cm) bound by mortar (cf. Ško-284). The thermal area was built in phase 1 in the second quarter of the 1st century AD. It was damaged by fire in the first half of the 2nd century AD and was after that renovated.

The 1st phase *frigidarium* basin in the apsis of room 3 was at that time reduced in size and the original coating was replaced by a new mortar layer (cf. samples Ško-318, Ško-294 and Ško-316). The bottom of the basin was probably covered with marble slabs, as can be deduced from rectangular imprints in the mortar; the same is valid also for the 1st phase basin (imprints and small remains of marble elements remain namely also in the 1st phase mortar). The *calidarium* (room 4) was similarly modified in phase 2B (cf. Ško-250, Ško-246 and Ško-170). Also in phase 2, channel structures in the western part of the terrace were built (damaging the original stone paving in the external western courtyard, to which sample Ško-284 relates) and the surface of the courtyard was raised. Only small additions and modifications were completed in the later phases in the thermal area (Figure 2) (Žerjal & Novšak, 2020).

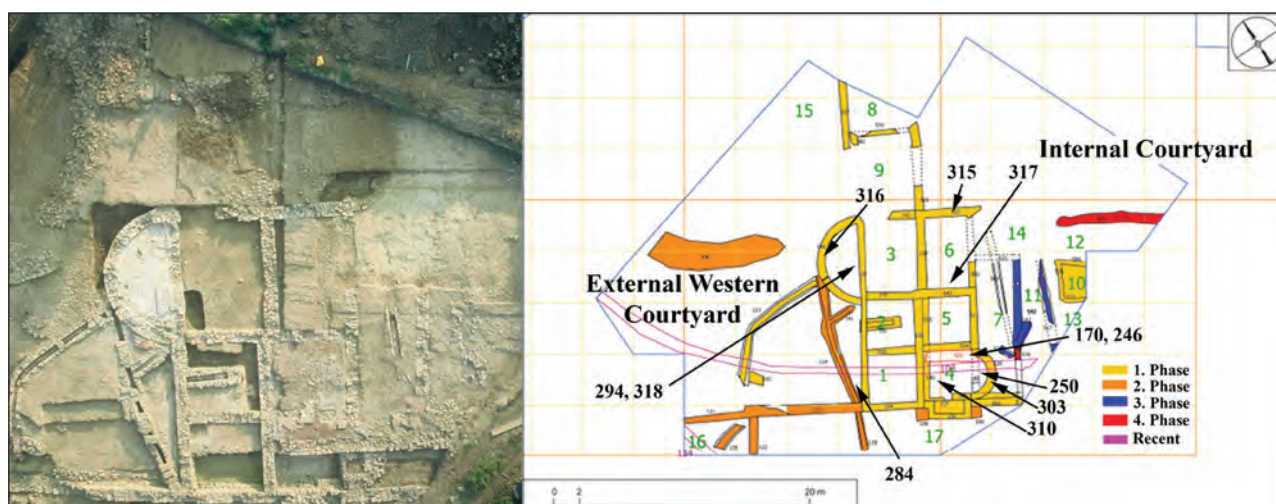


Figure 2: Aerial photograph (by O. Kovač, J. Krajšek, R. Urankar, archive Arhej d. o. o.) and plan (by T. Žerjal, Arhej d. o. o.) of the southern part of the villa with the thermal area.

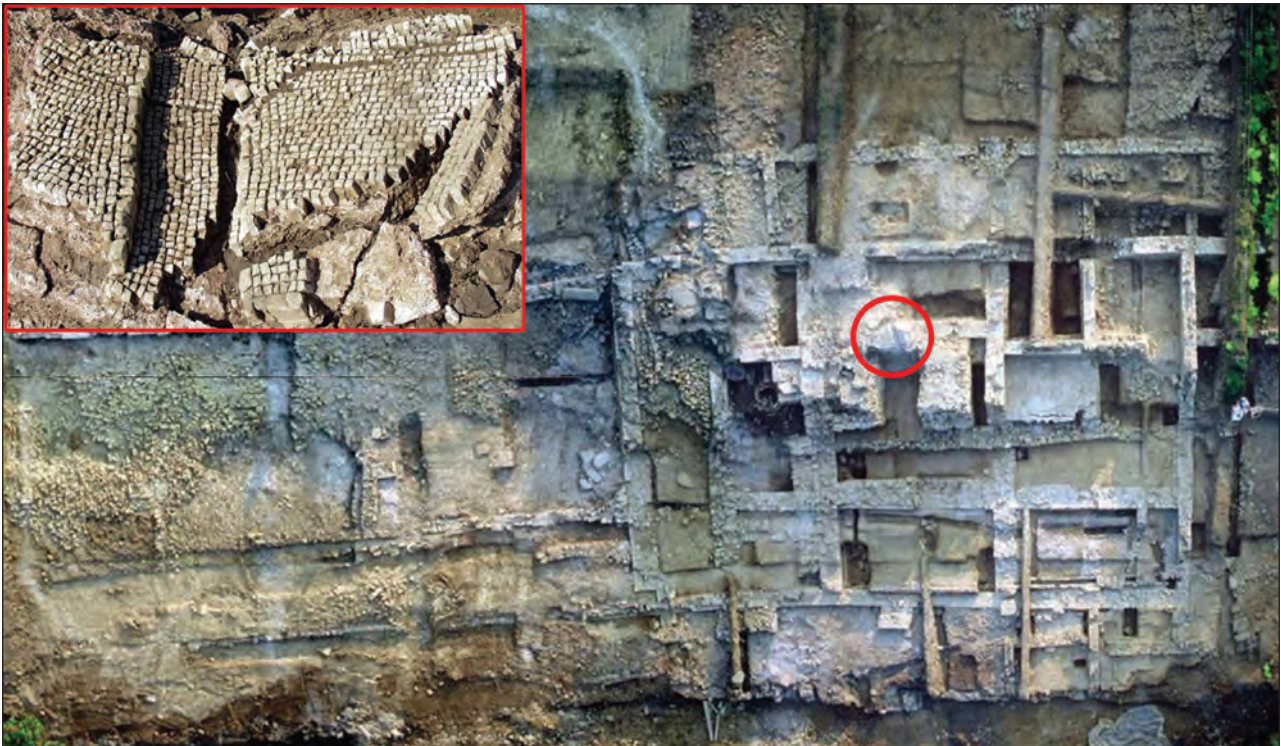


Figure 3: Aerial photograph of the north-eastern part of the villa with the productive area (by O. Kovač, J. Krajšek, R. Urankar, archive Arhej d. o. o.), the marked location of the torcularium channel (circle, detail in inset) between rooms G and L; sample Ško-239 was taken from the mortar bedding layer of the large tesserae mosaic of the channel belonging to this torcularium.

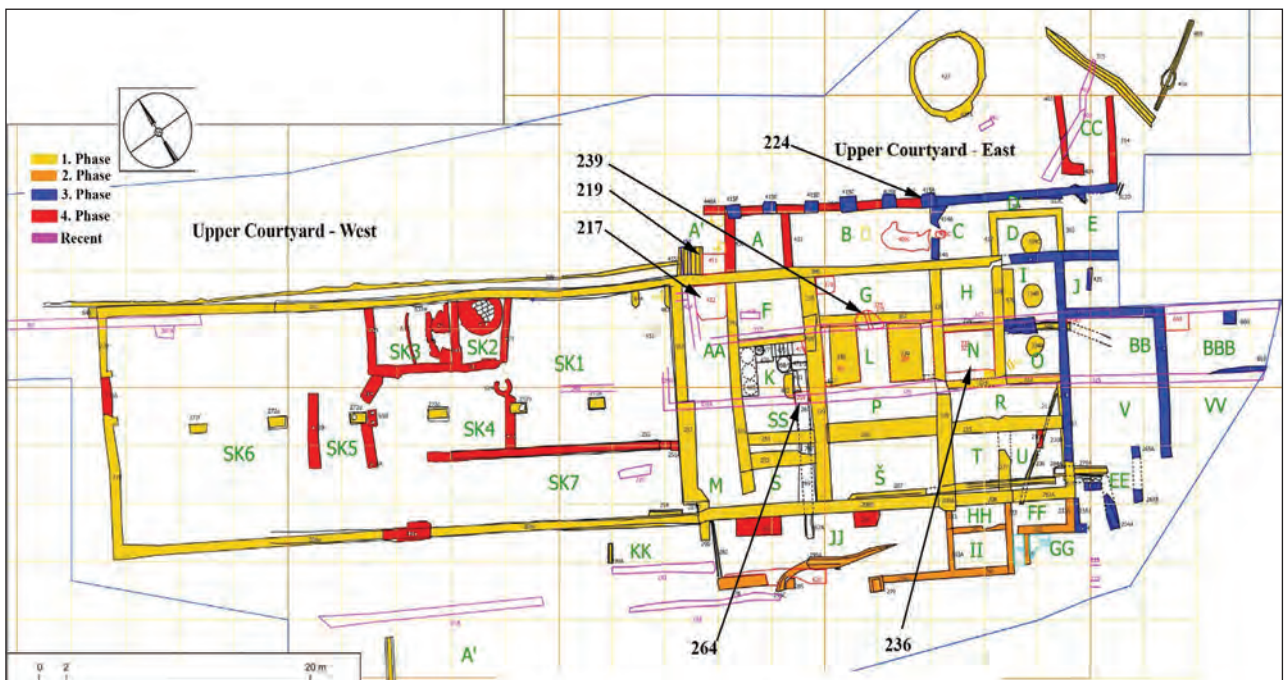


Figure 4: Plan of the north-eastern part of the villa with the productive area and an extensive storeroom to the west (by T. Žerjal, Arhej d. o. o.), with location of the samples.

Sample Ško-316 was sampled from the coating plaster of the apsidal basin in *frigidarium* 3 which was applied in phase 2B, dated to the 2nd century AD. Ško-318 and Ško-294 are taken from the mortar of the structure made of sandstone elements, composing the bench and the border wall of the smaller basin of phase 2B in room 3. From *calidarium* 4, but from the same phase, comes sample Ško-250, which represents mortar of a built platform (built to level up the 1st phase basin) in the apsis of room 4. Next to it a coarse terracotta mosaic, made of big rhomboid and trapezoid *tesserae* (5 x 3 x 2 cm), together with its preparatory layers was laid: Ško-246 is part of the lower, *rudus* layer (12 to 18 cm thick) and Ško-170 of the *nucleus* layer (10 to 15 cm thick).

The other samples come from the productive area in the north-eastern part of the upper terrace, shown in figures 3 and 4 above. This part of the villa was also built in phase 1 during the second quarter of the 1st century AD. It consists of an elongated building, stretching east-west, with sloping levels towards south. The western part of the building consists of a large storeroom with a central row of pillars (room SK* in Figure 4). The eastern part of the building hosts different units used for the production of wine, oil and possibly even flour. Sample Ško-239 is from the bedding layer of the large white *tesserae* mosaic of the channel belonging to the *torcularium*, a wine or oil press, located in rooms G and L (dimensions of the *tesserae*: 2,5 x 2,5 x 4,5 cm; dimensions of the *tesserae* on the border of the channel: 6 x 4 x 7 cm –with the longest dimensions referring to the vertical embedment height) (Figure 3 and inset). This kind of revetment for productive structures, such as *torcularia* is rare, but not exceptional, and it was probably also very effective in its use. A similar example of *torcularium* with mosaic coating is attested in room 3 of the Roman villa of Russi in north-eastern Italy (Mansuelli, 1962; Guarnieri, 2016, 33–34).

Ško-236 belongs to the mortar bedding layer of the *opus spicatum* pavement in room N which could be identified with the *lacus*, i.e. the must collection basin, which could be in that case related to the same press.¹

A similar sample is Ško-217, sampled from the mortar (3-5 cm thick) covering a low structure in room AA, which could also be identified with a productive arrangement or, alternatively, with a simple floor. Sample Ško-264 corresponds to the preparatory mortar layer of a white *tesserae* mosaic (*tesserae* dimensions: 1-1.5 x 1 x 2.5 cm) in room SS and includes a piece of *tessera*; the mortar layer was 3-4 cm thick and was laid over a drainage channel heading south.

North of the building, there was an open courtyard, from which water was collected through a drainage channel along the northern wall of the storeroom SK*. At the very eastern end of this channel, there was a stepped structure with steps made of sandstone slabs of

different length, 20-80 cm, and height, 8-12 cm, as well as depth, 10-20 cm. This is identified with a stepped cascade pertaining to the same water channel, with the stepped chutes used for reducing flow velocity (Chanson, 2000, 47–48). Mortar from between these steps was sampled and analysed (Ško-219). Small interventions can be dated to phase 2. In phase 3 (3rd century AD) the complex was extended towards east and north, with the creation of a porch (room AB) to the north; sample Ško-224 comes from the foundation structure of one of its pillars. This porch was transformed into two rooms in phase 4 (second half of the 3rd century AD), when also consistent interventions took place in order to transform and divide into several smaller rooms the western storeroom (Žerjal & Novšak, 2020, 26).

Analytical Procedure

Of the samples provided, the 19 that appeared to be most representative of the site were selected for further analysis. The wide variety of procedures described in the following sections was applied in a case-by-case manner in order to resolve specific questions, and therefore, as Tables 1 and 2 below show, not every sample was treated in the same way. The appropriate analytical procedure was determined by the (limited) available time and resources combined with a philosophical assessment of how much *additional* information could be gained from utilizing the full analytical “toolbox”; e.g. if there were two large fraction ceramic aggregate mortars, such as Ško-170 and Ško-239, only one was produced into a polished thin section and analysed by costly methods such as SEM-EDX, FTIR-i and TGA. Thus, of the 19 samples discussed here, the main focus was made on 12 that were prepared as polished (uncovered) petrographic thin sections (shown in light blue in Tables 1 and 2), as well as sample Ško-310 prepared as a highly polished cross-section. Of these, 5 were selected as an important subset (with the analytical procedure shown with bold X's) to which the entire gamut of procedures would be applied, answering in particular the questions of level of hydraulicity of these mortar samples – an important quality in assessing the original intent of the artisanship and thus the functionality of the archaeological object.

Optical Microscopy

The preliminary step of mortar analysis typically involves a selection from the provided samples in order to pick the ones that will tell the most complete story of an archaeological site. Often, observation of a mortar sample by cutting and visual inspection (referred to as “hand section” above) will inform the researcher about the future course of analysis. For this site, the samples Ško-246, Ško-317 and Ško-318 were observed to not be

¹ About the Roman wine production method, also from an experimental point of view cf. Indelicato, 2020.

Table 1: Sample description and preparation.

Sample Name	Room/Phase	Mortar Type	Sample Preparation
Ško-101.1	N.D.	Wall Painting	Pol. Thin Section
Ško-101.2	N.D	Wall Painting	Pol. Thin Section
Ško-170	4/2B	Cocciopesto	Cross Section
Ško-246	4/2B	Ceramic Piece, from rudus	Pol. Thin Section
Ško-250	4/2B	Cocciopesto	Pol. Thin Section
Ško-284	7/1	Cocciopesto	Cross-Section
Ško-294	3/2B	Lime-sand	Cross-Section
Ško-303	4/1	Lime-sand	Pol. Thin Section
Ško-310	4/ pre-1	Cocciopesto	Cross-Section
Ško-315	6/1	Lime-sand	Pol. Thin Section
Ško-316	3/2B	Cocciopesto	Pol. Thin Section
Ško-317	5/1	Tuff Piece, from stone paving	Pol. Thin Section
Ško-318	3/2B	Tuff Piece, from structural mortar	Hand Section Only
Ško-217	AA/1	Cocciopesto	Pol. Thin Section
Ško-219	A/1	Lime-sand	Pol. Thin Section
Ško-224	C/3	Lime-sand	Pol. Thin Section
Ško-236	N/1	Cocciopesto	Cross-Section
Ško-239	G-L/1	Cocciopesto	Pol. Thin Section
Ško-264	SS/1	Cocciopesto	Hand Section Only

mortar, but rather large ceramic (-246) or tuff (-317 and -318) aggregates with a small amount of mortar attached. Because of this, they were excluded from the analytical process². Following this, microscopy was performed on the mortars, with the majority of the results being based on petrographic examination of 11 of the polished thin sections.

Petrography was performed by a combination of 2 different optical microscopes. The first was a Nikon SMZ 1500 transmitted light, stereomicroscope (SM), with an 8x eyepiece, 1x lens, and the ability to zoom from 0.75x to 11.25x, for a range of magnification from 6x to 90x. It includes two attachments: an incident light source (with either direct or raking light) and a rotating polarizer film. The second was an Olympus BX40 polarizing light microscope (PLM) with a 10x eyepiece and 5,10,20,50 and 100x objectives, for a range of magnification of 50-1000x. Both the incident and transmitted light sources are polarizable. With both microscopes, a Cannon EOS 600D DSL camera coupled with the EOS

Utility software was used to capture photomicrographs. Preliminary results from optical microscopy allowed for the further categorization of the mortar samples (shown in Figure 5 below); more in-depth analysis is discussed in the following Results sections, which includes the estimation of the volumetric binder to aggregate ratio (b:a) of each thin sectioned mortar by the application of image analysis in the form semi-automatic pixel-area counting of pseudo-coloured photomicrographs by the Adobe Photoshop® software (discussed in Section 3.3) (per Mertens *et al.*, 2009).

SEM-EDX

The second image-based step of the analytical protocol employed was the examination of the thin sections by SEM-EDX. These tools were used primarily to understand the chemical nature of areas of interest, such as potential reaction rims on ceramic aggregate, and to visualize such areas at high magnification. Analysis by

² Ško-317 was selected as one of the 12 samples for thin sectioning, both to confirm its nature and to open up the possibility of further analysis of the tuff used at Školarice, to be addressed in the conclusions section.

EDX was of particular importance to perform oxide percentage analysis of relic lime clasts in order to determine the source of lime binder, as well as to determine the level of hydraulicity of the mortars' binder matrix. For the latter, both area and point by point measurements were made in order to determine the relative proportions of silica plus alumina oxides to calcium oxide ($\text{SiO}_2 + \text{Al}_2\text{O}_3 / \text{CaO}$), this is shown as a percentage and referred to as the "hydraulicity index" (HI) (Boynton, 1980, Elsen *et al.*, 2010). This is the first of four methods by which the HI was determined (see Table 3, Section 3.5). The device used for this work was a FEG Quanta 250 Scanning Electron Microscope (FEI, U.S.A.) coupled with a Pegasus APEX Energy-Dispersive X-ray spectroscope (Ametek EDAX, U.S.A.) equipped with the Genesis SEM Quant software (SEM-EDX). Images were generally taken in back-scattered electron mode (BSE) at 20 kV with a spot size of 3.5-4.0 nm and a working distance of between 12-15 mm. EDX measurements were typically quantified by oxide analysis (omitting carbon, heavily prevalent in the epoxy resin), so that results are to be understood to represent the proportion of one oxide to another in the target area.

Fourier-transform Infrared Spectroscopy Imaging (FTIR-i)

The final step of the image-based analysis protocol relied on using FTIR-imaging to map the area corresponding to cement hydrates in the polished thin section, in this case calcium-aluminosilicate-hydrate (C-A-S-H) resulting from the pozzolanic reaction (Mehta, 1987). The target spectra for defining these molecules correspond to the detection of carbonates (CO_3 ; stretching around 1350 cm^{-1} to 1500 cm^{-1} , silicates (Si-O stretching between 1100 and 950 cm^{-1} and a hydrate band at ca. 1660 cm^{-1} indicating the interstitial bound (or "crystal") water of C-A-S-H (Baragona *et al.*, 2019a; 2019b; Baragona, 2021; Diekamp *et al.*, 2010; Farcas & Touzé, 2001; Horgnies *et al.*, 2013; Hughes *et al.*, 1995; Paama *et al.*, 1998; Yu *et al.*, 1999); the detection of these species at the same locations in the mortar are taken to indicate co-molecularity (*ibid*). By selecting these bands, the software automatically displays the distribution of the intensity of such bands across the entirety of the image. A colour scale from red (strong) to blue (absent) indicates the distribution of the selected bands, which corresponds to the distribution of chemical species. Combining this information with a scaled image of the mortar creates a pseudo-coloured image of the mortar thin section from which pixel-counting can again be used, this time to determine the percentage of the surface area of the mortar's binder in which C-A-S-H is detected, thus the volumetric content of C-A-S-H in the binder matrix, a direct visualization of a mortar's hydraulicity (Baragona *et al.*, 2019a; 2019b). Put simply, this step combines detection by FTIR-imaging (Yu *et al.*,

1999; Diekamp *et al.*, 2010) with image analysis techniques (Mertens *et al.*, 2009) by way of comprehensive imaging. This is the second way by which the hydraulicity index was calculated (see Table 3, Section 3.5), and is illustrated in Figure 6 below.

The device used was a Nicolet iN 10 MX Infrared Imaging Spectrometer (Thermo-Fischer Scientific, USA), with cooled MCT-A linear array detector, and interfaced with OMNIC Picta software. Spectra were collected in reflection mode, spectral range $4000\text{-}720 \text{ cm}^{-1}$, aperture $25 \mu\text{m}$, with 8 cm^{-1} spectral resolution, and spatial resolution $<10 \mu\text{m}$. Normal mapping mode was used with a 2 second collection time per step. The spectra were finally vector normalized and baseline corrected.

Chemical Dissolution per RILEM TC-167

Traditional, laboratory-based mortar dissolution testing was performed in parallel to the image-based analysis, in a large part to determine if there was a correlation between results gained by both methods. Two test procedures from the RILEM technical committee publication on the characterization of old mortars (TC-167-COM Sections 2.1.1 and 2.1.1.3, Method 2) were selected to characterize the archaeological mortars (Middendorf *et al.*, 2005). First, the mortar was dissolved in hydrochloric acid, separating the binder from the aggregate, thus defining the binder to aggregate ratio gravimetrically (see Table 4). Second, the quantity of soluble silica was determined by treating the remnants of the previous test with a boiling alkali solution, which separates the hydraulic phases from the remaining mortar components. The results of this test are also expressed gravimetrically (see HI Table 3) and represent a third method of determining the HI (soluble silica as a percentage of the total soluble binder). These two sets of results were refined by testing the aggregate separately from the mortar, to determine the aggregates' solubility in acid and alkali. While these dissolution tests provide gravimetric data, the image-based analysis provides volumetric data, which will be considered when drawing conclusions from these data sets in the Results Section 3.5.

Thermogravimetric Analysis

Thermogravimetric analysis (TGA) is a common method used to study historical mortars, in particular to analyse the binder content (Paama *et al.*, 1998; Bakolas *et al.*, 1998; Drdácý *et al.*, 2013; Moropoulou *et al.*, 2000; 2004); it was the fourth method by which the HI was determined for this work. This method allows for both the identification and gravimetric quantification of various contents of the mortar. The components typically measured are free water until $105 \text{ }^\circ\text{C}$, bound water and organic material between $150\text{-}600 \text{ }^\circ\text{C}$ and calcium carbonate starting at $700 \text{ }^\circ\text{C}$. The identification/ quantification of C-A-S-H is related to

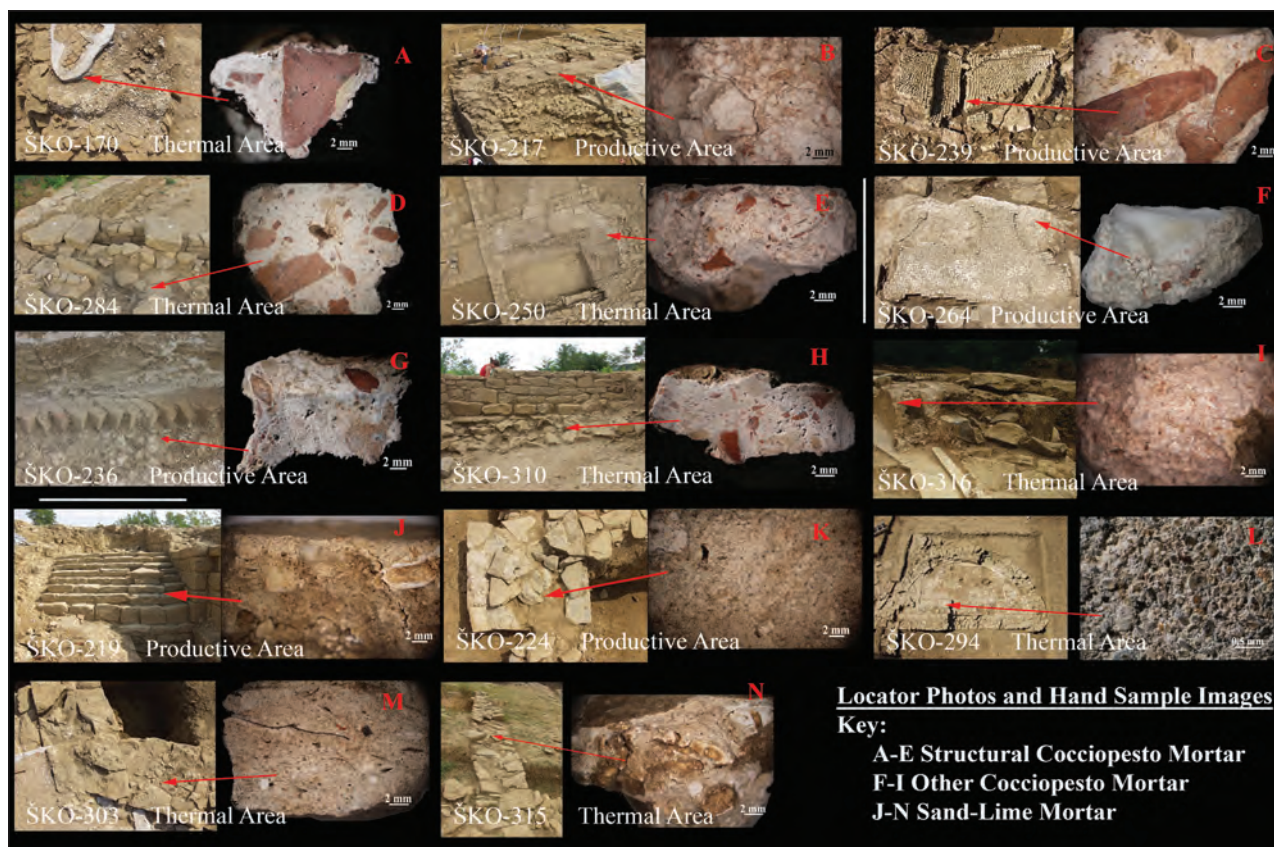


Figure 5: Photos and hand-sample images of the mortars discussed (excludes wall painting and non-mortars). A-E: Ško-170, Ško-217, Ško-239, Ško-284; Ško-250; F-I: Ško-264, Ško-236, Ško-310, Ško-316; J-N: Ško-219, Ško-224, Ško-294, Ško-303, Ško-315 (field photographs: Arhej d. o. o.).

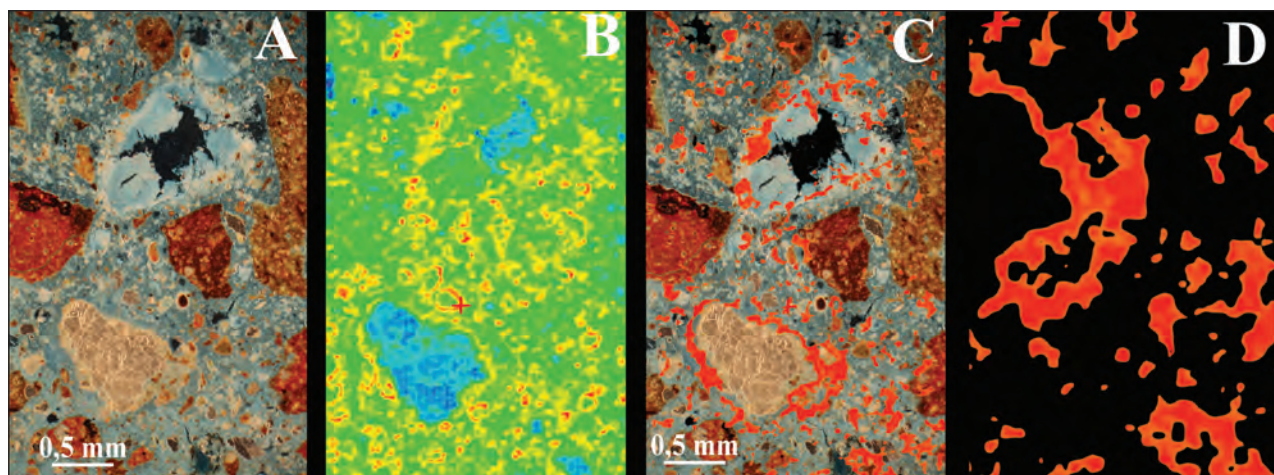


Figure 6: Illustration of the FTIR-imaging technique to determine mortar binder content, per Baragona 2019; 2021. Left to Right: A) SM, transmitted light, darkfield mode image of a cocciopesto mortar (Ško-316); B) FTIR-image of the same mapping the co-molecular carbonate (wavenumber 1410 cm^{-1}) and silicate (wavenumber 955 cm^{-1}) likely indicative of C-A-S-H, note distinctive occurrence at aggregate rims; C) Scaled composite image with peak intensities of the images wavenumbers superimposed over the SM image from 1); D) Detail of area of binder imaged through FTIR-i, scaled with background removed for automatic pixel counting to give a surface area percentage, calculated as a percentage of the surface area of the binder given in the HI results below.

the detected bound water content (*ibid.*). Components can be identified by the temperature at which they leave the system, signified by “peaks” in the thermograph corresponding to the weight loss their leaving causes. Because there can be overlap between peaks, there is some room for interpretation by the operator, however there is often the additional confirmation by mass spectrometry.

Five of the archaeological specimens (Ško-217, Ško-239, Ško-250, Ško-310, Ško-316) were gently crushed in a porcelain mortar and sieved through a 0.063 mm sieve to separate the binder from the aggregates before analysis. The rich-in-binder fraction was subjected to thermal analysis. Thermal analysis was performed using a TA Instruments Discovery SDT Q650. Approximately 20 mg of the sieved fine fraction of the sample was placed in alumina pans. The analysis was performed in a nitrogen atmosphere within the temperature interval from 25 to 1000°C with a temperature gradient of 20°C per minute. The calcium carbonate content and water bound in hydrated phases (CSH, CAH), was quantified as interpreted by the Universal Analysis 2000 software. The results were converted into a percentage (weight loss by dehydration of hydrated phases/ total binder weight loss = weight loss hydrated phases + carbonated phases = decimal result *100 for percentage) for comparison to the HI results given by the three other methods; most importantly to correlate to the results given by FTIR-imaging in combination with digital image analysis on the same 5 samples (Results Section 3.5).

RESULTS

The thirteen samples examined scientifically fall into one of 3 types: finish or decorative mortar (samples 101.1, 101.2, 303 and 219), structural mortar (samples 217, 224, 239, 310, and 315) or waterproofing mortar (samples 250 and 316), while samples 246 and 317 proved to not be mortar. Many samples include ceramic material, which could generally be considered a pozzolan or reactive aggregate; these are samples 217, 224, 239, 250, 310 and 316 of the structural and waterproofing mortars as well as the base “rough coat” of the wall painting fragments sample 101.1. The two waterproofing mortars show a much finer fraction of ceramic material. This would have produced a more strongly hydraulic mortar and perhaps a smoother (and therefore more aesthetically pleasing) finish. Samples 170, 264 and 284, although not analysed scientifically, would appear to be most similar to the ceramic-bearing structural mortars in terms of composition and application. The imagery and discussion in the following Sections 3.1-3.4 describe all of the mortars analysed in a comprehensive way, Section 3.5 that follows provides multi-analytical data pertaining specifically to the level of hydraulicity found in 5 *cocciopesto* mortars, and what this information implies for the interpretation of the site in terms of its construction and archaeological history.

Lime Binder and Relict Clasts

Large, partially burned pieces of calcareous stone can be found throughout the samples; it can be reasonably assumed that these are remnants of the source stone for the lime (“relict lime clasts”) (Hughes *et al.*, 2001). Evidence of calcination is shown by PLM as areas where there is undispersed lime near relict lime clasts (Figure 9, C, D), or nearly fully burned relics that preserve some micro-features of the original stone (Figure 7, Right). These are predominately marble, which is not locally available, but was apparently used as lime source stone from the 1st building phase onwards and also in the wall mortar sample 310 of the structure predating the construction of the villa. All of the *cocciopesto* mortars, the sand-lime mortar samples 219, 224 and 294 as well as both wall painting mortars contain these marble relics (although 294 appears to have both these as well as limestone relics). The marble used in the *intonaco* layers of the wall painting fragments (samples 101.1 and 101.2) matches this marble as well, both optically/structurally (by OM – Figure 7) as well as chemically (by EDX). Samples 303 and 315, pertaining to phase 1, appear to have a different source of raw material, a sandy limestone, which may be of local provenance. It is interesting to note that the *cocciopesto* mortars from this and later construction phases use marble as the lime source stone, while these sand-lime samples appear to have a different source.

In all cases except for the wall painting fragments, the presence of large, undispersed lime lumps can be seen as evidence for a “hot” or rapid slaking technique (Pintér *et al.*, 2011; Weber *et al.*, 2013; 2014). For Roman era *cocciopesto* or pozzolanic mortar a “basket slaking” technique was often employed that would leave these lumps as well (Adam, 1994; Hughes *et al.*, 2001; Elsen, 2006; Baragona, 2021). The *intonaci* of the wall painting fragments lack lumps indicating the use of lime putty. Only two samples (219 and 303, again pertaining to phase 1) contain pieces of charcoal (lime production fuel residue), indicating generally thorough sieving of the quicklime after production, a clean burning wood, or both. The wood species appears to be a softwood (conifer). Preliminary EDX results of both relict lime clasts and undispersed lime lumps reveal a nearly pure (95%+) calcium carbonate composition, again with the exception of samples 303 and 315 in which the sandy limestone relics could include up to 15% silica and alumina by oxide percentage. The limestone was not found to be dolomitic. Additional photomicrographs of the lime binder source stone are shown in Figure 8.

Aggregates and Classification

Petrographic examination of the 12 thin sections allowed for the classification of the mortars, which as presented was done by aggregate type, but could have

Table 2: Analysis performed by sample. Blue-highlighted samples used in Table 3.

Sample Name	OM	SEM-EDX	FTIR-i	Chem.-Diss.	TGA-DSC
Ško-101.1	X	X			
Ško-101.2	X	X			
Ško-170	X			X	X
Ško-246	X	X			
Ško-250	X	X	X	X	X
Ško-284	X			X	X
Ško-294	X				
Ško-303	X	X		X	
Ško-310	X	X	X	X	X
Ško-315	X	X			
Ško-316	X	X	X	X	X
Ško-317	X	X			
Ško-318	X				
Ško-217	X	X	X	X	X
Ško-219	X	X		X	
Ško-224	X	X			
Ško-236	X				
Ško-239	X	X	X	X	X
Ško-264	X			X	X

also been done by mortar function. The former method was chosen to help frame the later discussion regarding binder hydraulicity (of the *cocciopesto* mortars) found in Sections 3.5 and the Discussion. Grouped this way, there were four *cocciopesto* mortars and four sand-lime mortars; the remaining four thin sections consisting of the two wall-painting stratigraphic mortars and two “non-mortars” are discussed in following sections.

In four of the samples (217, 239, 250, 316) plus the base layer of sample Ško-101.1, the predominate aggregate is ceramic material (see Figure 9A-D, K). Low burned ceramic material was commonly used in Roman times as a pozzolan to create a mortar that was both durable and had the ability to set in moist environments, per Vitruvius (Secco *et al.*, 2018; also see Vitruvius II.5.1). Larger pieces of ceramic were often used in sub-flooring, such as a hypocaust or in sample 239 (Figure 9B), a preparation layer for a mosaic drain channel of a *torcularium* press, dated to phase 1. The ceramic material itself appears in two different colours, reddish and yellowish (sometimes greenish because of intrusion of the blue dye). This is more likely due to differing firing

temperatures rather than different clay sources, as EDX shows a similar oxide composition throughout, and SEM shows similar microfeatures in all samples. Sample 224 also shows a large piece of ceramic perhaps used to help fill a crack in the surrounding masonry as the mortar itself is composed of sandy aggregate, as well as a few loose foraminifera (Figure 9F).

At Školarice, *cocciopesto* mortars were used in a wide variety of applications. Samples 250 and 316 (Figure 9C, D), both pertaining to phase 2B, i.e. a renovation phase (following fire), but from two different rooms of the thermal area, contain mostly finely graded ceramic aggregate and were applied as bedding, waterproofing or a rendering coat; of the samples not prepared as thin sections, number 310 (Figure 9H above) is of similar composition. The remaining samples include a wider range of ceramic sizes and appear to have more of a structural application (as a flooring or subflooring mortar), such as the previously mentioned sample 239, and the analogous (non-thin sectioned) samples 170, 236, 264, and 284 shown in Figure 5 A, D-F. The connection between the ceramic grading, their application and their

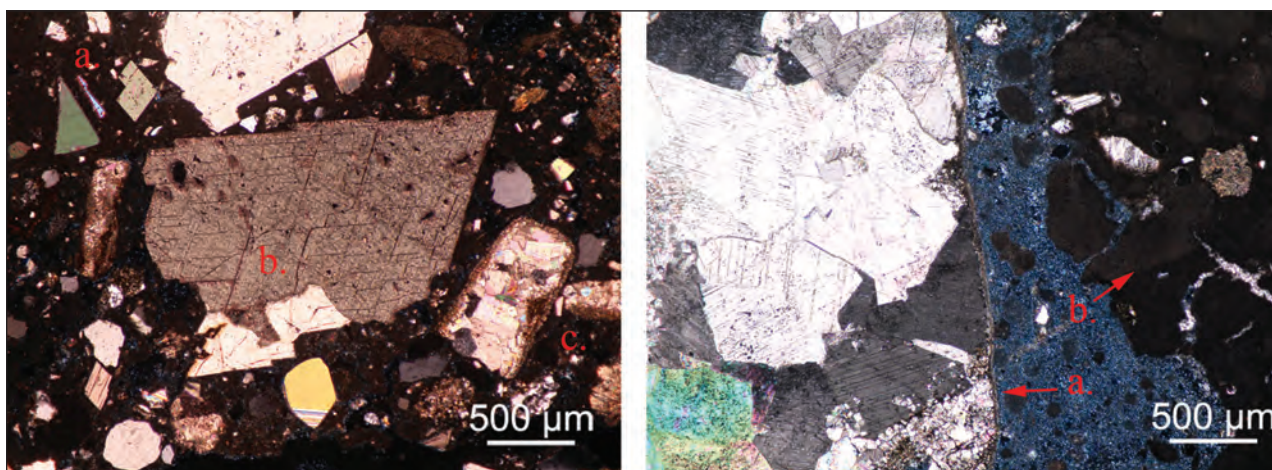


Figure 7: Školarice Intonaco, Lime Source Stone Left Image: Marble fragments used in the middle intonaco layer of sample Ško-101.1. While smaller fragments (a.) may indicate the use of sparite, the larger, polycrystalline fragment (b.) contradicts this. (c.) shows a weathering frontier around another multi-crystal fragment, indicating the marble's exposure before (likely) reuse. Right Image: Large marble fragment in the binder of sample Ško-239 (a.) and corresponding partially burned lime relic clast (b.) with corresponding large grain boundaries indicative of the original cleavage. Both: PLM-Trans. Light, crossed polars.

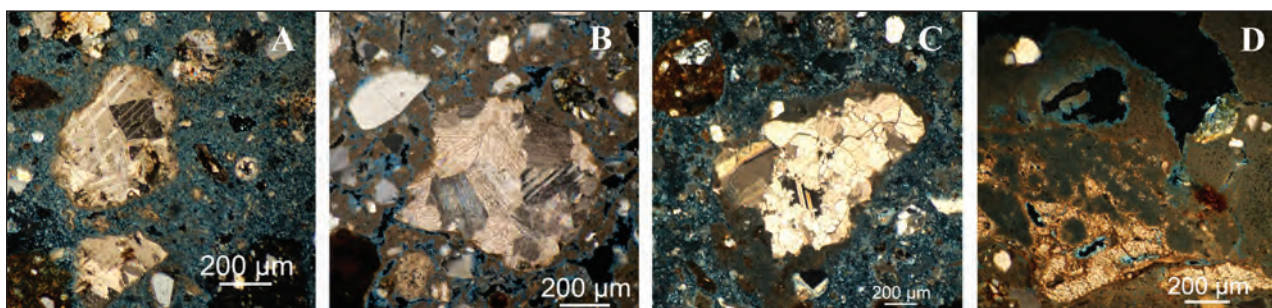


Figure 8: Školarice Lime Lump Examples Left to Right: A) Marble relict, sample 219 (lime-sand mortar); B) Marble relict, sample 250 (cocchiopesto mortar); C) Marble relict with attached undispersed lime containing brick dust, sample 316 (cocchiopesto mortar); D) Sandy limestone relict with undispersed lime above, sample 315 (lime-sand mortar); all PLM-Trans. Light, crossed polars.

apparent binder hydraulicity is discussed in Section 3.5 below.

The remaining non-wall painting samples are composed of sand-lime mortar; the sand is composed of both silicate and carbonate material and the angularity is typical for sand coming from a small river. The aggregates appear to be nearly all the same size, (“well sorted”), but it is not clear if this is the result of sieving or was natural at the source (Figure 9E-H).

Samples 101.1 and 101.2 (Figure 9K, L) are wall painting fragments found at Školarice, but cannot be associated with a specific building phase, as they were found within rubble layers in the thermal area. Sample 101.1 is a mortar of at least 6 layers (rough coat, 2 arriccio layers and 3 intonaco layers in which the final finish was white. A 6th lime wash layer is at the top surface,

blended with the final intonaco layer composed mostly of lime with small fragments of marble. This is followed by 2 more layers of lime-marble intonaco, with the aggregate size quickly increasing. The sample broke during preparation, not along the intonaco–arriccio boundary, but rather through an arriccio layer. The base layer is highly porous and composed of a mixture of ceramic material with some large calcareous pieces, perhaps unburned lime source stone. Sample 101.2 consists of at least 3 layers. The lack of ceramic material in the base layer indicated that this wall covering was probably not in a room that maintained a moist environment, although it is possible the sample does not include all layers. The top intonaco layer was coated with a layer of yellow ochre. Large lime lumps are prevalent in the lower layers.

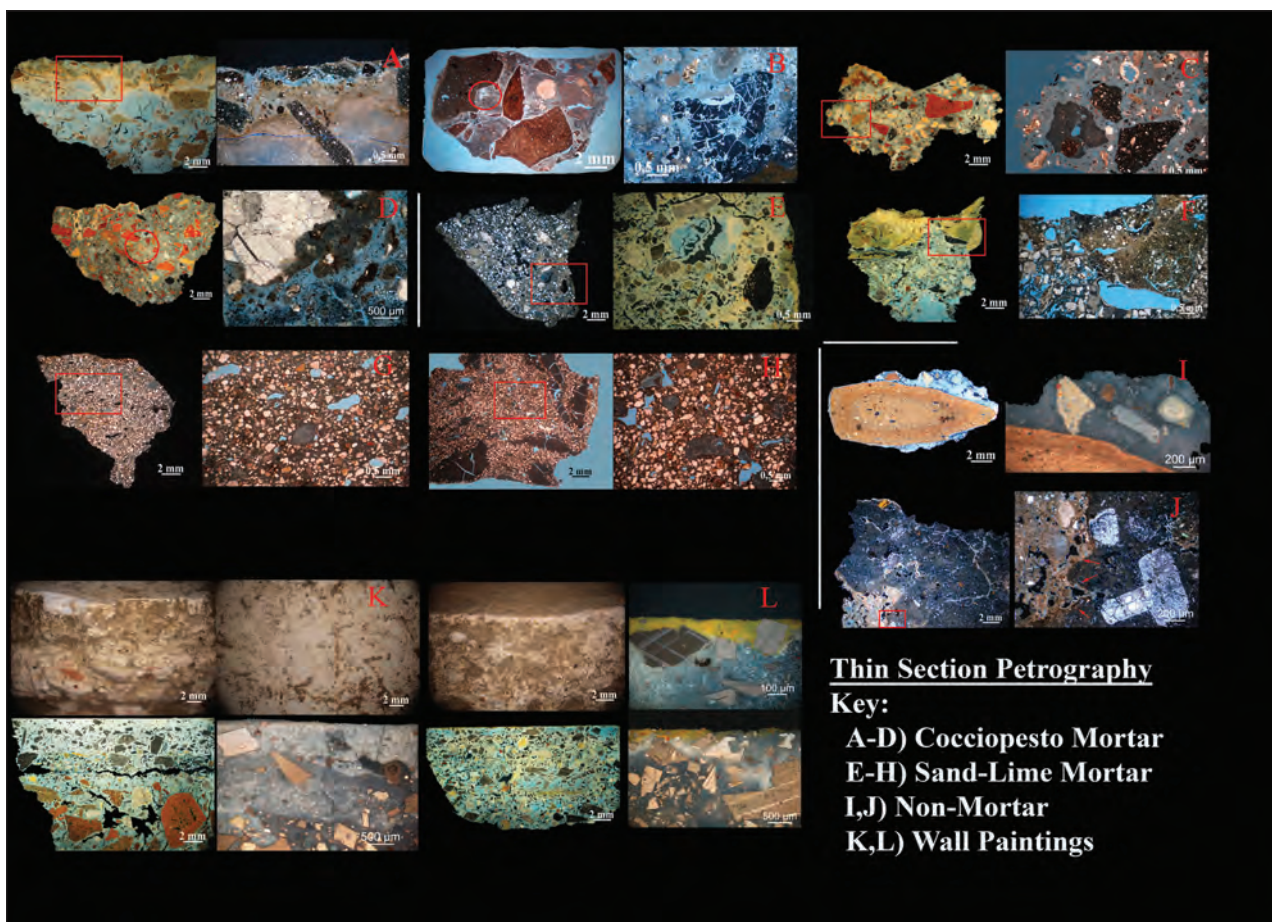


Figure 9: Školarice Petrographic Images: stereomicroscopy (some in dark-field mode) and polarizing light microscopy with descriptions as in the text below.

Finally, samples 246 from the *rudus* layer in room 4 (Figure 9I) and 317 from the stone paving in room 5 (Figure 9J) represent examples of what are likely pieces of fill with small amounts of mortar attached, 246 dominated by a large piece of ceramic and 317, a large piece of tuff. Although they were not examined in detail, 246 may simply be a fragment of a structural mortar with a large, apparently unworked ceramic aggregate, and 317 may be of further interest since tuff is not a locally sourced stone. It appears to be a piece of an ashlar, rather than added as an aggregate, and does not appear to be pozzolanically active (and is not a small enough grain to be so).

Binder to Aggregate (b:a) and Porosity Results

Pseudo-colour images of photomicrographs of a representative area of each mortar prepared as a polished thin section were analysed by point-counting in image editing software (Adobe Photoshop) in order to determine the binder to aggregate ratio (b:a) and porosity (by volume) as described in Section 2.2.1 above; the b:a

was also determined gravimetrically through chemical dissolution as a comparison as described in Section 2.2.4 above. Examples of images produced this way are shown in Figure 10 below. The results of this analysis are given on a sample by sample basis in Table 4 in the Summary below, but in general there was little difference in b:a between mortar type, regardless of analysis type. The cocciopesto mortars have volumetric b:a ranging between 2:3 to 2:1 (40%-67% binder, average 52%, standard deviation of 13.5%), while the sand-lime mortars have a b:a ranging from 3:5 to 2:1 (37.5%-67% binder, average 48%, standard deviation 14%). The gravimetric results are similar with average b:a of 54% (Std Dev. 17%) and 45% (Std Dev. 6%) for mortars with ceramic or sand as aggregate, respectively.

The porosity as determined by image analysis was more divergent; the average porosity of sand-lime mortar was 8% (range 2–14%, Std Dev. 5.6%), while the average porosity of cocciopesto mortar was half as much at 4% (range 1.6%–7.1%, Std Dev. 2.6%). Thus, while both mortar types used a similar amount of lime binder, the cocciopesto mortars were found to be more compact.

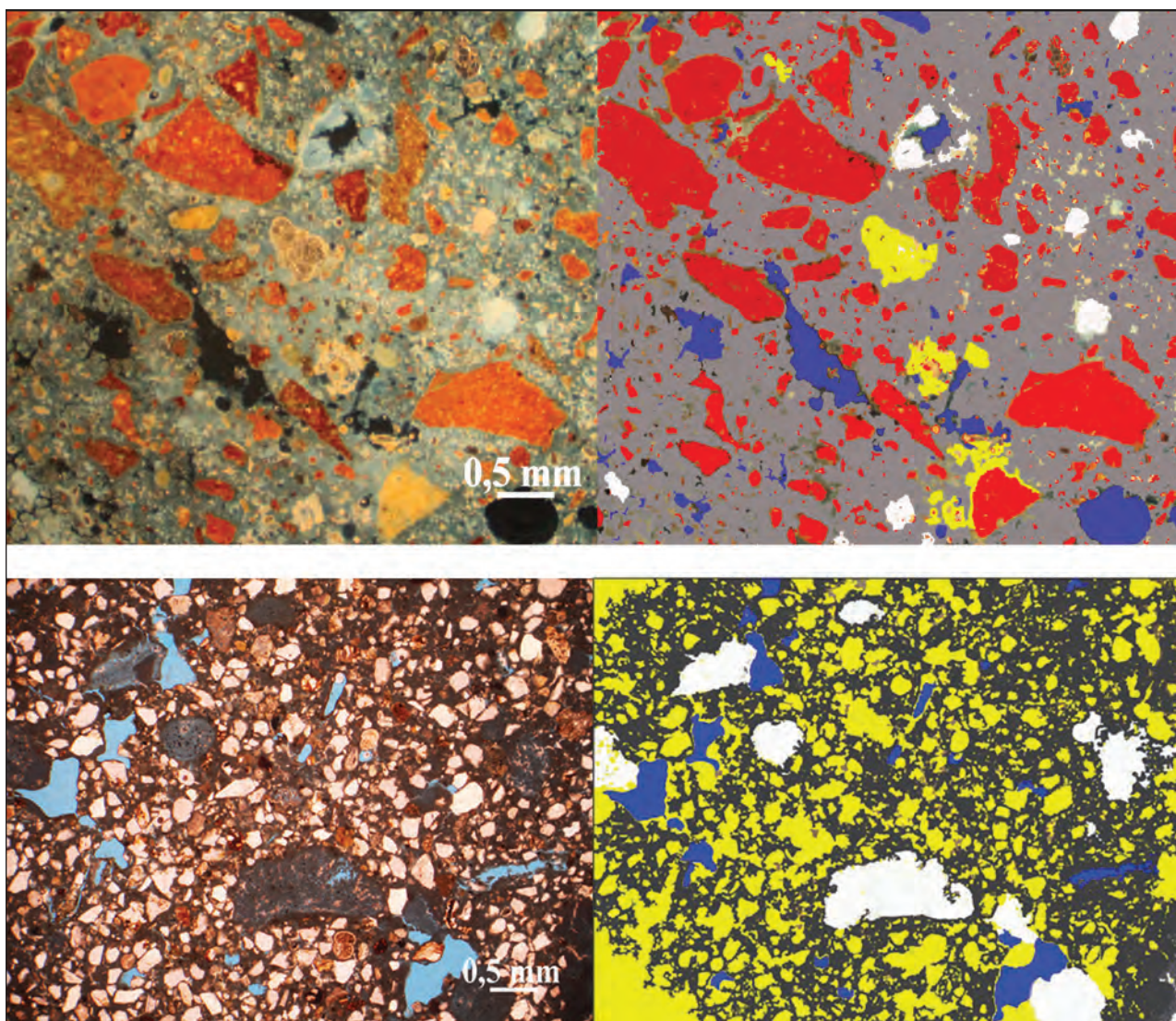


Figure 10: Examples of a cocciopesto (above) and sand-lime (below) mortar as pseudo- coloured for b:a and porosity quantification.

SEM-EDX RESULTS

In general, the SEM was used sparingly for analysis of this archaeological site; the EDX function proved to be more useful in determining or confirming the chemical composition of relic lime clasts and lumps, as well as the content of the binder matrix. The results of the former (lime lumps) have already been discussed in Section 3.1 above, while the discussion of the oxide content of the binder matrix will be discussed in Section 3.5 below. Figure 11 below displays images that show the utility of the SEM.

In the first two images (Figure 11A, B), more detail is gained on the nature of the wall painting mortars, such as determination of stratigraphy and identification of pigments. In Figure 11A there is a clear carbonation line between the last layer of intonaco and a layer of

whitewash. The large bright objects in Figure 11B are the yellow ochre pigment particles visualized. Figure 11C confirms the presence of the product of the pozzolanic reaction, displaying small relics of C-A-S-H (needle-like growths) in the crack of an undispersed lime lump, while Figure 11D highlights a (rare) piece of fuel residue. Figure 11E shows a phenomenon that was so unique and noteworthy that EDX mapping was used to investigate the formation of magnesium silicate hydrate, as described further in Figure 12 below. Figure 11F shows a detail of the weathering rim on a piece of marble used in the intonaco for Ško-101.1, indicating that the marble used for both this layer and the lime source for many of these samples was likely recycled (hence the weathering front indicating previous usage/exposure). The last two images (Figures 11G, H) show

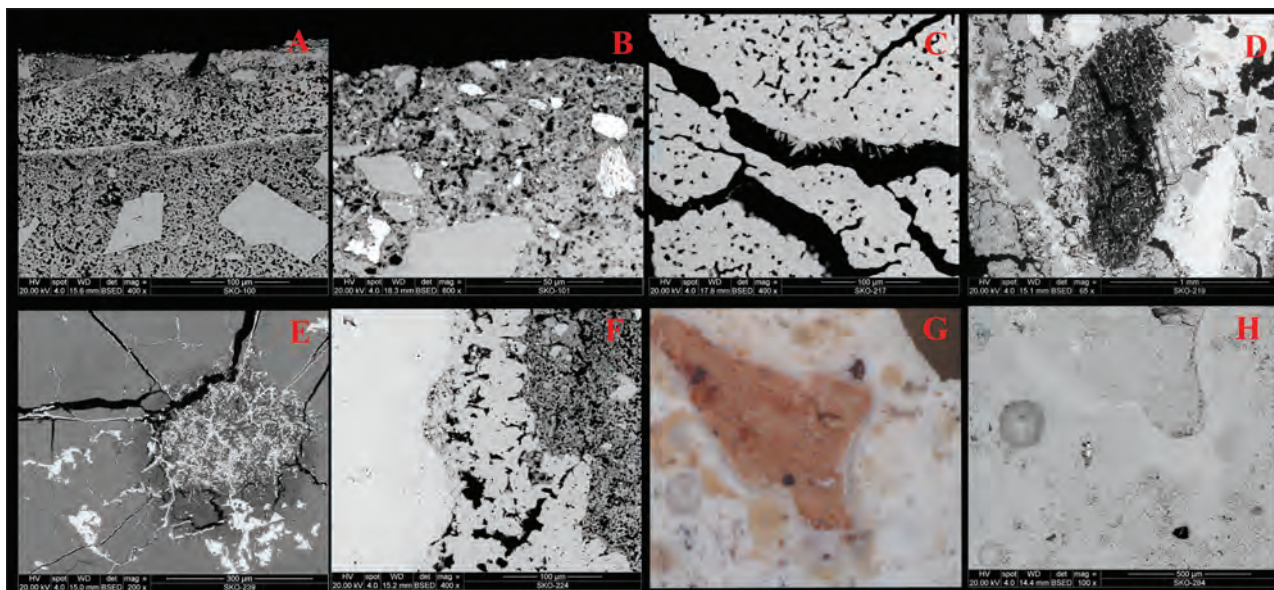


Figure 11: Various phenomena visualized in greater detail by SEM, as described in text.

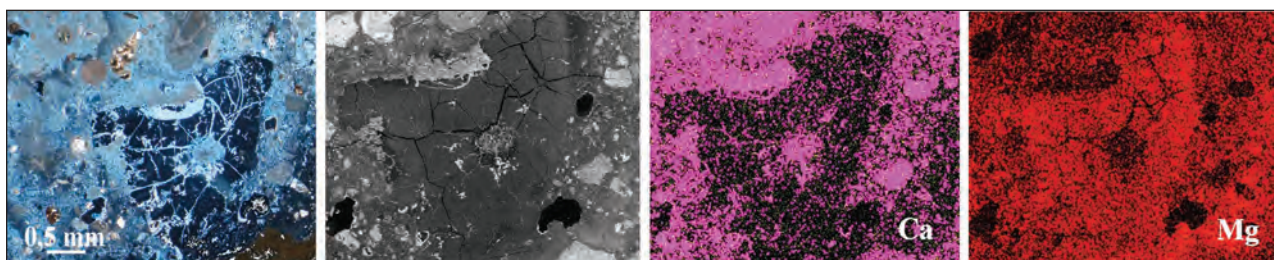


Figure 12: EDX mapping results (left two images) for a magnesium-rich, calcium-poor area of the binder in sample Ško-239.

what can be misconstrued as a reaction ring on a piece of ceramic, but closer inspection shows it to be an area where lime binder has compacted in the space near the rim of a ceramic piece *without* reacting with it.

Figure 12 shows an area of Ško-239 that by petrographic examination, presented itself as a strange, glassy area of the binder near a large piece of ceramic aggregate (as shown in the cross-polarized photomicrograph in this figure). This area was further examined using EDX mapping when point analysis indicated the presence of large amounts of magnesium, but no calcium (or silicon) was present at this location. Although only one example, this area could be the remnants of part of a binder system composed, at least in part, by magnesium-silicate hydrate, a binder (by-)product of recent scholarly interest when found in Roman-era mortar (Secco *et al.*, 2020). Since the lime source stone used in the mortar was not found to be dolomitic, and it can be assumed that seawater was not used in its slaking, the source of the magnesium, and if this can be found elsewhere on the site is a source of potential further study.

Multi-analytical Results Determining the Hydraulicity Index

Special emphasis was given to the determination of the degree of hydraulicity (in this case, pozzolanicity) of five of the mortars found at Školarice in order to examine if particular structures had been built with the need for particularly strong or waterproof mortars in mind, since the type of mortar employed by ancient builders gives evidence of their intent for the structure in which it was employed. In the context of ancient Roman sites, the addition of ceramic to lime mortar was used in a wide variety of applications to improve the qualities of the mortar (Vitruvius II.5.1; VII.1.3; VII.4.1), taking advantage of the pozzolanic reaction to create a hydraulic mortar. Although the reddish hue of the binder of these mortars is taken as empirical evidence that this was done, and indeed as evidence of pozzolanicity, the steps outlined in Sections 2.2.2-2.2.5 above were performed to provide correlative, quantitative

Table 3: Hydraulicity index results by technique.

Sample Name	HI by: Chem.	HI by: EDX	HI by: TGA	HI by: FTIR-i
Ško-217	.08	.09	.16	.06
Ško-239	.21	.25	.20	.20
Ško-250	.13	.22	.25	.15
Ško-310	.21	.30	.16	.25
Ško-316	.25	.50	.21	.31

evidence of the pozzolanicity/hydraulicity of these mortars, referred to herein as their hydraulicity index (HI). Thus, were EDX, FTIR-i, chemical dissolution and thermal gravimetric analyses made of the binder of these five mortars, with the results given in Table 3. The data for the 5 samples are generally consistent based on all four analytical procedures, with the 3 examples with more finely graded ceramic material having on average, a higher hydraulicity index. Except for sample 217, all could be described as moderately hydraulic, which in the case of 239, from the *torcularium* channel, is somewhat unexpected given the dearth of visible small aggregates. As for 217 the low hydraulicity index could be important for determination of the function of the mortar and structure to which it belonged, as it was not clear from the archaeological context. Possible interpretations include either a productive arrangement or a raised floor structure, with the latter option as more plausible in light of the analytical results presented herein. In relation to 250 and 316, hydraulicity was expected because of the archaeological context of the thermal area they come from. This was not the case for sample 310, which came from the wall of an earlier building predating the construction of the villa. Since very little remained of this structure, any additional information, such as the use of a hydraulic mortar is therefore very precious and can be useful for its further interpretation. Figure 13 shows the clustering of results by sample, with the EDX and FTIR-i results having the strongest correlation and TGA as a clear outlier. There is no difference in observed hydraulicity between the samples of different building phases, although this assertion would benefit from the analysis of a larger number of samples.

DISCUSSION

Concluding, 19 mortar samples were analysed, 12 prepared as polished petrographic thin sections. These came predominately from 2 building phases,

but from different types of structures. Samples were selected with the aim to include mortars with ceramic or pozzolanic aggregates, with hydraulic features: they were chosen by macroscopic inspection based on their pinkish colour or observable reddish and blackish grains. Analytical results revealed that macroscopic identification is often not reliable. For example, sample 239 has a higher hydraulic index than sample 217, even though the former displays only large ceramic inclusions and whiteish binder, yet was still found to be moderately hydraulic, while the latter is pinkish with fine ceramic aggregate present. Sample 317, as well as others not included in this work, include tuff, but show no reactivity, hence are not pozzolanic.

A summary of the results of this analysis is given in Table 4 below. Overall, they are remarkable for their consistency with typical Roman building materials and practices of the era. There are several findings that illustrate this. Firstly, the use of marble for both the intonaco layers of the wall painting fragments as well as its (re-)use as the predominate source stone for the production of quicklime in all types of mortars, despite the fact that there is no locally available marble, while limestone can be found in the region. This implies the import of marble specifically for this use or its recycling from previous, earlier structures, from the site or surroundings. The latter option is still more interesting, considering that small portions of an older building predating the construction of the villa were found in place. In the mortars of the 1st phase, it appears that marble was burned for quicklime, but only used in cases when it would be combined with ceramic material to make a pozzolanic mortar; those using sand aggregate appear to use quicklime calcined from local limestone (see Figure 8 above). This adheres generally to the rule laid out by Vitruvius that harder stone should be used for mortars used in structural applications (Vitruvius II.5); the lesser presence of marble in the 1st phase implies that the material was in this early phase hard to acquire, but was nevertheless selected for structural uses that required waterproofing as well. This leads to the second point, that in both most investigated phases (1 and 2B), particular care was taken to produce a robust waterproofing material when making flooring (samples 217, 239) or waterproofing mortars (samples 250, 316); this was not done in samples of structural mortar used outside (sample 315).

As to the methodology used in determining these conclusions, the petrographic and scanning electron microscopic images speak for themselves; the ability to determine conclusive, correlative results that identify mortar constituents and their relation to one another is the primary advantage of the study of thin sections (Elsen, 2006; Baragona *et al.*, 2019a;

Table 4: Summary of results by sample prepared as thin section.

Sample Name	Mortar Type	Binder Type	Binder Hydraulicity	Aggregate Type	B:A Gravimetric	B:A Volumetric	Macro-Porosity Volumetric
Ško-101.1a	Rough coat	Air Lime	Weakly Hydraulic?	Mostly ceramic	N.D.	1:1 (.5)	16.2%
Ško-101.1b	Arriccio	Impure Air Lime	Non-hydraulic	Crushed marble / river sand	N.D.	1:1 (.5)	9.3%
Ško-101.1c	Intonaco	Air Lime	Non-hydraulic	Nearly pure lime	Nearly pure lime	Nearly pure lime	N.D.
Ško-101.2a	Arriccio	Impure Air Lime	Non-hydraulic	Mixed	N.D.	2:3 (.4)	10.8%
Ško-101.2b	Intonaco	Air Lime	Non-hydraulic	Crushed Marble	N.D.	2:1 (.67)	5.7%
Ško-217	Cocciopesto	Lime + Ceramic	Feebly Hydraulic	Mostly ceramic	.42	2:3 (.4)	2.4%
Ško-219	Drainage Render (Exterior)	Air Lime	Non-hydraulic	Silicate + Carbonate Sand	.36	3:5 (.375)	14.8%
Ško-224	Masonry mortar	Air Lime	Non-hydraulic	Silicate + Carbonate Sand	N.D.	3:5 (.375)	10.2%
Ško-239	Cocciopesto	Lime + Ceramic	Moderately Hydraulic	Mostly ceramic	.43	2:3 (.4)	1.8%
Ško-250	Waterproofing	Lime + Ceramic	Moderately Hydraulic	Ceramic and relic clasts	.80	3:2 (.6)	5.7%
Ško-303	Wall Render	Air Lime	Non-hydraulic	Silicate + Carbonate Sand	.44	2:1 (.67)	2.2%
Ško-310	Masonry mortar	Lime + Ceramic	Moderately Hydraulic	Mostly ceramic	.55	N.D.	N.D.
Ško-315	Masonry mortar	Air Lime	Non-hydraulic	Silicate + Carbonate Sand	N.D.	1:1 (.5)	5.1%
Ško-316	Waterproofing	Lime + Ceramic	Mod. – highly Hydraulic	Mostly ceramic	.52	2:1 (.67)	7.1%

2019b). Comparing the two methods of determining the binder to aggregate ratio (detailed in 3.3 above) proves that the method of using pseudo-colouring thin section micrographs is a good analogue for the results found by chemical dissolution, while one should use caution when comparing gravimetric to volumetric data; the results given in Table 4 show values that are similar enough to support this assertion (i.e. there is never a case where the values are drastically different).

The novel technique of using scaled FTIR-image results to determine the hydraulicity index of archaeological mortars shows similarly promising results. The results of the methods given in 3.5 above are compared by means of a scatter chart in Figure 13 below, where the results of analysis of 5 selected ceramic-lime (theoretically pozzolanic) mortars by

the four complimentary methods are shown, listed from left to right by sample with the highest observed average hydraulicity index. Clustering the results shows that by and large, the techniques are comparable, e.g. all 4 methods show sample 217 to be the least hydraulic and 316 to be the most hydraulic, with the others falling in between when the values given by each technique are averaged. Thus, they are likely to be interchangeable in terms of determining how hydraulic a mortar is relative to another one, even if the results given this way are not in the truest sense quantitative. True outlier results are only given by the TGA and EDX results, and only in one instance each. Future studies can therefore likely give good results by just one or two of the above complementing techniques, saving time, money and other resources.

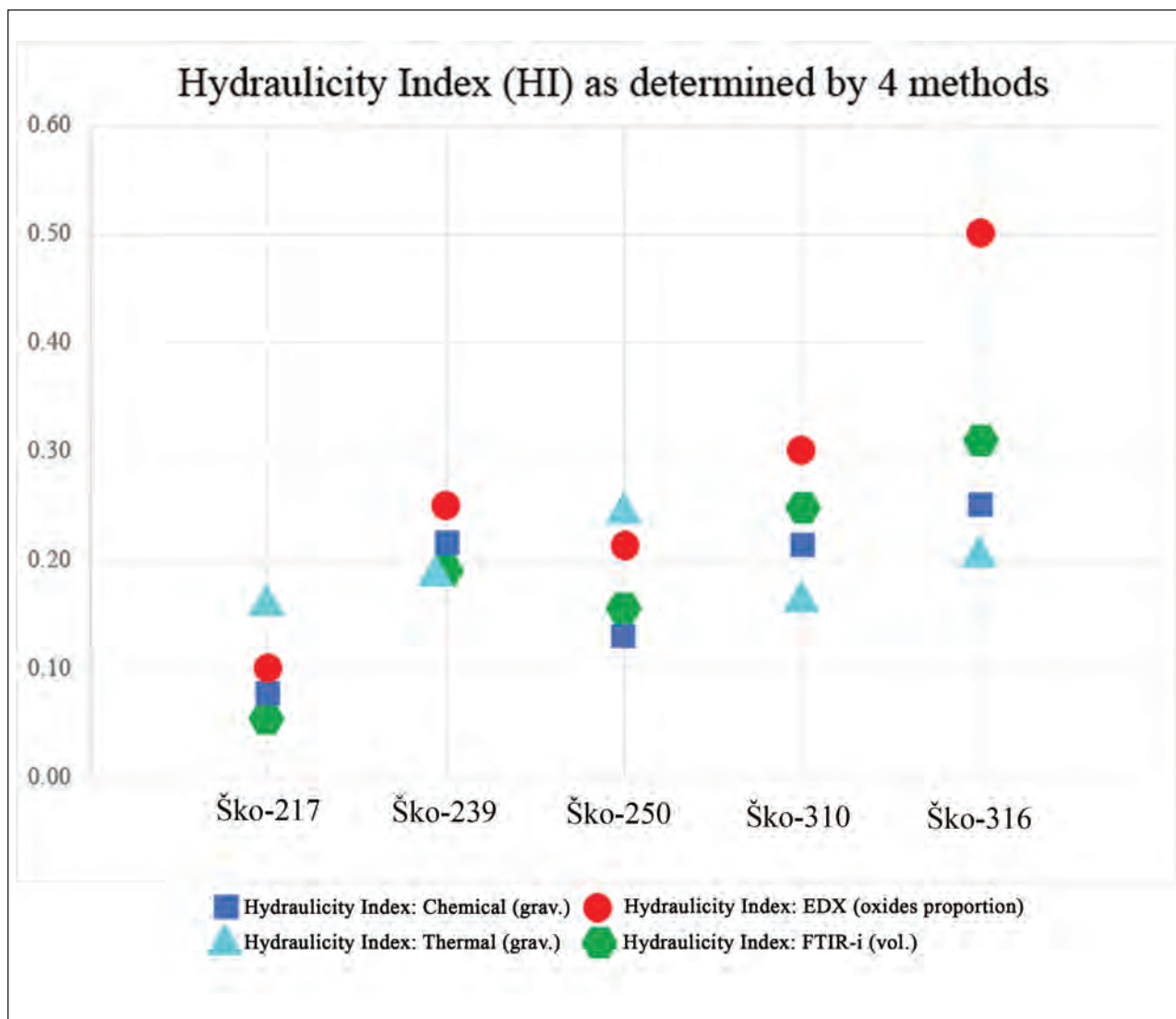


Figure 13: Results of four different, complementary methods for determining the hydraulicity index of a pozzolanic mortar. Key: Green – FTIR-i, Dark Blue – Chemical Dissolution, Light Blue – TGA, Red – EDX oxide percentage.

CONCLUSIONS

This case study provided the opportunity to prove the efficacy of a novel method of determining the hydraulicity index of a mortar by FTIR-i on polished thin sections. This method is invasive, but non-destructive (of the sample) and therefore could be used in cases when there is not enough sample material (or the resources) to make both a thin section and perform chemical or thermal dissolution. All 4 techniques (FTIR-i, SEM-EDX, TGA-DSC and chemical dissolution) are good for determining the hydraulicity index, i.e. pozzolanicity of a mortar. The techniques of TGA and chemical dissolution are destructive. SEM-EDX is not, but it is both more expensive and less definitive than FTIR-i. SEM-EDX shows that the minerals associated with pozzolanicity are in the same

location, while FTIR-i indicates the co-molecularity of the types of silica and carbonate (and sometimes hydroxide) associated with pozzolanicity (Brunello *et al.*, 2019; Baragona *et al.* 2019a; Baragona 2021).

In general, hydraulic mortars were given special attention in research, as they are particularly helpful in determining or confirming the use of a structure. In the Roman era, these mortars were often used in areas of high humidity or in direct contact with water, such as flooring or the walls of baths or cisterns (Adam, 1994), but also productive areas, kitchens, courts and gardens or other areas exposed to the elements as porticoes and facades.

In the case of Školarice, the material destined to be analysed as examples of hydraulic mortars of the site, was in the first step selected because of its function and

context, secondly by optically observing the samples, which were recognized as potential hydraulic mortars for their pale pink colour, due to the presence of crushed brick or of greyish granules hypothetically identified as pozzolana. Here presented analyses show that only a part of them were actual hydraulic mortars. This shows that criteria frequently used by archaeologists on site to identify hydraulic mortars do not comply with reality, and hydraulicity has in fact always to be tested.

The Roman villa at Školarice provides an interesting case study of early Imperial Roman architecture, built over successive building campaigns with a high level of sophistication. A wide range of well-established and the above-mentioned novel analytical technique showed the skillful use of different mortar recipes for a wide variety of applications at this Roman villa, which was probably also a waystation with baths that was additionally a center of agricultural production.

As mentioned before, the villa is arranged on two terraces, with completely different functions, on the lower terrace an elegant thermal complex is arranged, the other one hosts a productive storage area. Analysis showed that mortars of both areas were prepared with similar attention and sophistication, also with regard to the hydraulicity of the mortars, what we would necessarily expect, being one the typical ambience of hydraulic mortars and high-quality architecture and decoration (i. e. baths), the other a space of functional character only tangentially connected to “wet” production activities.

In some cases, the analysis provided important hints for determining the specific purpose of a structure. This was the case of sample Ško-217, sampled from the mortar covering a low structure in room AA, which was tentatively identified either with a productive arrangement or, alternatively, with a simple floor. The low hydraulicity index of the sample makes the latter option more plausible, especially when compared to the hydraulicity index of sample Ško-239, which pertains to a typical productive arrangement, the *torcularium*.

Similarly, the moderate hydraulicity of sample Ško-310 must be pointed out: the sample came from the wall of an earlier building predating the construction of our villa. Rare structural remains (as well as plaster fragments and some small finds) of this earlier building were identified in the thermal area and the use of a hydraulic mortar in its walls could indicate, that also this earlier building had already a similar function.

In this sample, but also in other samples dating from the 1st phase onwards, marble (which is not locally available) was predominately used as lime source stone, whereas mortars with sand aggregate Ško-303 and Ško-315 pertaining to phase 1 showed to have (probably local) sandy limestone as a source of raw material for lime production. The more selective use of marble in the 1st phase implies that the material was at this time (second quarter of the 1st century AD) hard to acquire, but was specially chosen for structural uses

that also required waterproofing. The import of marble in the area of north-western Istria was in Roman times generally very rare, as architectural decoration and sepulchral monuments show here predominantly to be made of limestone from Aurisina / Nabrežina (north-eastern Italy), and only singular marble elements are documented (Krašna, 2022, 44).

On the other hand, the indiscriminate use of marble as a source for lime production in phase 2B (dated to the 2nd century AD) seems to show its wider accessibility. However, sample Ško-294 taken from the structures of the basin in room 3 of the thermal area renovated in phase 2B, stands here out as it shows both marble and limestone as lime source stones. This would indicate that also in phase 2B, limestone was still used for this purpose, but was detected more rarely because there are fewer samples representing this building phase.

Also the sand-lime mortar Ško-224, the only sample pertaining to phase 3 (3rd century AD), includes marble relics, as well as ceramic material, but is at the same time non-hydraulic, showing that marble was used as a lime source from the very first building of the site, predating the construction of our villa, throughout the 1st and 2nd building phases and also until the 3rd one, and this seems to represent a very characteristic feature of this site.

Crushed marble is also used in the intonaco layers of the wall painting fragments (samples Ško-101.1 and Ško-101.2) and they match the marble used as lime source optically/structurally and chemically. A weathering rim on a piece of marble used in the intonaco for Ško-101.1 indicates that the marble used for both this layer and the lime source for many of the samples was likely recycled. This implies that disused marble material was imported for this use, or it was recycled from an adjacent earlier structure. The latter option is still more interesting, considered the older building predating the construction of the villa mentioned before.

At the same time, marble slabs and some other marble features were used especially in the thermal area of our site from the 1st building phase onwards. As they were not sampled for this analysis, we cannot confirm, if they also pertain to the same marble quality. But, in the area of north-western Istria the site of Školarice seems to represent an area of special concentration of marble materials, some of which used as raw material for lime production and as an aggregate in mortars, some as slabs and cornices (Žerjal & Novšak, 2020, 77, 231–232, 578); parts of a statue of Dionysus dating to the first half of middle of the 2nd century AD were used in the wall of room SK4, created in the area of the large storehouse during the 4th building phase (this is during the second half of the 3rd century AD) (Žerjal & Novšak, 2020, 134, 204, 632, 633). This concentration of marble materials at this site could as well support the above-mentioned theory that the villa also functioned as a *mansio* (“*Aquae Risani*”) on the route of the

main public road *Via Flavia*, being in this way better connected to the partially centralized logistics of the marble trade.

The intonaci of the wall painting fragments lack any lumps indicating the use of lime putty. Two samples (Ško-219 and Ško-303, pertaining to the 1st phase) contain pieces of charcoal, which we can recognize as lime production fuel residue. In all other samples, the quicklime was apparently thoroughly sieved after production or a clean burning wood was used, or of course both (cf. on this Laycock *et al.*, 2018). The wood species appears to be a softwood, or conifer. Research about paleo-vegetation is still very rare, but the presence of conifers in this area in Roman times could be indicated by the analyses made by Metka Culiberg (1997, 136–137), however to a quite limited extent. It would be also possible that the wood was not necessarily of strictly local provenance but was imported from other nearby areas. This could have been done for construction, with leftover pieces being used as fuel for lime production.

The lime was very likely produced locally and in fact the remains of a lime kiln were excavated near the villa, at Križišče. The lime kiln was located along the road leading from the main road *Via Flavia* to the villa. Individual limestone pieces, which are not from the immediate surroundings, were found in the filling of the kiln and were meant to be burnt to lime. Another filling layer contained burnt earth, charcoal, limestone, and lime remains. Roman pottery was found in the fill as well, but remains of charred wood found inside the firing chamber were radiocarbon dated between 650 and 820 AD (Novšak *et al.*, 2019, 81–82; Kutnar, 2022, 28–31). Despite this, excavators of the site considered this dating apparently incorrect, as they concluded that the lime kiln was used for the construction of the Roman villa at Školarice (Žerjal & Novšak, 2020, 21), where also a round structure for mixing mortar from the 1st building phase was found in the upper courtyard (cf.

Figure 4, round structure north of the productive area). Inside this structure, ample remains of lime could be documented (Žerjal & Novšak, 2020, 378). These lime remains, both from the lime kiln and from the structure for mixing mortar, were not sampled for this analysis, but will be subject of research in the near future. As mentioned previously, marble was found to be the main source stone for the lime at Školarice, so (containing the lime kiln remains of limestone) it is likely that the radiocarbon dating is correct. Considering the location and Roman finds in it, it is also possible, that the lime kiln was established for the construction or later renovations of the Roman villa and then reused in post-Roman time.

Open questions that could provide more detail into the case of the Roman villa of Školarice and its building materials, involve the provenance of the marble and sandy limestone source stones used for lime production, as well as the tuffaceous material used as paving mentioned above. Additionally, analysis of any organic material that has left traces in the stone or soils of the site, e.g. GC-MS on oils or tannins soaked into the rough stone mosaic of the *torcularium* could be used to conclusively determine the usage of the productive arrangement.

ACKNOWLEDGEMENTS

The authors would like to thank Farkas Pintér at the Austrian Federal Office for Monuments (Bundesdenkmalamt) for the use of his SEM-EDX as a back-up and to corroborate the results of the device mentioned in this work. The authors are also thankful to Maša Sakara Sučević at the Regional Museum of Koper and to Matjaž Novšak from Arhej d. o. o. for allowing us to perform this research. Special thanks go to Tina Žerjal from Arhej d. o. o. for providing photographs and plans from the excavation and for several fruitful discussions. The authors acknowledge the financial support from the Slovenian Research Agency (research core funding No. P6-0247).

ARHEOMETRIČNA ANALIZA MALT Z RIMSKE VILE RUSTIKE NA ŠKOLARICAH (SLOVENIJA)

Anthony J. BARAGONA

Univerza uporabnih umetnosti Dunaj, Inštitut za konservatorstvo, Salzgies 14/1, 1013 Dunaj, Avstrija
e-mail: tonybaragona@gmail.com

Katharina ZANIER

Univerza v Ljubljani, Filozofska fakulteta, Oddelek za arheologijo, Zavetiška 5, 1000 Ljubljana, Slovenija
e-mail: katharina.zanier@ff.uni-lj.si

Dita FRANKOVÁ

Češka akademija znanosti, Inštitut za teoretično in uporabno mehaniko, Prosecká 809/76, Prague 9-Prosek, Republika Češka
e-mail: frankeova@itam.cas.cz

Marta ANGHELONE

Univerza uporabnih umetnosti Dunaj, Inštitut za konservatorstvo, Salzgies 14/1, 1013 Dunaj, Avstrija
e-mail: marta.anghelone@uni-ak.ac.at

Johannes WEBER

Univerza uporabnih umetnosti Dunaj, Inštitut za konservatorstvo, Salzgies 14/1, 1013 Dunaj, Avstrija
e-mail: johannes.weber@uni-ak.ac.at

POVZETEK

V prispevku so predstavljeni rezultati analize malt, uporabljenih pri gradnji rimske vile rustike na Školaricah v Sloveniji. Analiziranih je bilo 19 vzorcev iz različnih mikrolokacij in faz, še posebej dvanajst vzorcev, ki so bili pripravljene kot polirani petrografski zbruski. Ti vzorci so bili zaporedoma analizirani z optično mikroskopijo (OM), skenirno elektronsko mikroskopijo skupaj z energijsko disperzivno rentgensko spektroskopijo (SEM-EDX) in infrardečo spektroskopijo s Fourierovo transformacijo (FTIR-i), kar je omogočilo celovito analizo širokega spektra značilnosti in, kar je pomembno, kako so med seboj povezane. Posebna pozornost je bila namenjena reaktivnosti agregata in viru veziva apna. Določitev indeksa hidravličnosti veziva malte je pomemben kriterij pri oceni historičnih malt. Določili smo ga za keramično-apnene malte najdišča, in sicer s štirimi različnimi metodami (ki smo jih tako lahko tudi primerjali glede na dosežene rezultate): kemičnimi analizami z raztapljanjem vzorca, termogravimetrično analizo – diferenčno dinamično kalorimetrijo (TGA-DSC) ter analizo površine veziva z EDX in FTIR-i na ustreznih zbruskih. Pri slednji so bili spektralni podatki analizirani z analizo digitalne slike, ki je dala kvantitativne volumetrične rezultate, kar predstavlja novo tehniko za določanje hidravličnosti veziva za malto. S slikovnimi tehnikami smo določili tudi razmerje med vezivom in agregatom in poroznost. Rezultati so pomembno prispevali k interpretaciji vile, zlasti v zvezi z obsegom uporabe keramičnih frakcij kot pucolanskega ali hidroizolacijskega materiala.

Ključne besede: Rimska vila, Školarice, historična malta, FTIR spektroskopija, hidravlični indeks

SOURCES AND BIBLIOGRAPHY

Adam, Jean Pierre (1994): Roman Building: Materials and Techniques. London, Routledge.

Bakolas, Asterios, Biscontin, Guido, Moropoulou, Antonia & Elisabetta Zendri (1998): Characterization of Structural Byzantine Mortars by Thermogravimetric Analysis. *Thermochimica Acta*, 321, 151–160.

Baragona, Anthony, Weber, Johannes & Marta Anghelone (2019a): A Map is Worth a Thousand Pictures: Using FTIR-imaging to Analyze Petrographic Thin Sections of Historical and Experimental Mortar. In: Álvarez, José Ignacio, Fernández, José María, Navarro, Íñigo, Durán, Adrián & Rafael Sirera (eds.): Proceedings of the 5th Historic Mortars Conference, 19–22 June 2019. Bagneux, RILEM Publications SARL, 482–494.

Baragona, Anthony, Weber, Johannes & Farkas Pintér (2019b): Ein Bild sagt mehr als tausend Worte: historische Mörteltechnologie von der Antike bis ins 20. Jahrhundert. In: Herm, Christoph, Merkel, Stephen, Schreiner, Manfred & Rita Wiesinger (eds.): Archäometrie und Denkmalpflege 2019. Metalla Sonderheft 9. Bochum, Deutsches Bergbau-Museum, 129–132.

Baragona, Anthony (2021): Pozzolan-lime Mortar: from Antiquity to Present: On the Utility of Comprehensive, Image-based Analysis and Experimental Archeology for Understanding Historical Mortar. Doctoral dissertation. Vienna, University of Applied Arts.

Bosio, Luciano (1991): Le strade romane della Venetia e dell'Histria. Padova, Studio Editoriale Programma.

Boynton, Robert S. (1980): Chemistry and Technology of Lime and Limestone. New York, John Wiley & Sons.

Brunello, Valentina, Corti, Cristina, Sansonetti, Antonio, Tedeschi, Cristina & Laura Rampazzi (2019): Non-invasive FTIR Study of Mortar Model Samples: Comparison among Innovative and Traditional Techniques. *The European Physical Journal Plus*, 134, article number 270.

Chanson, Hubert (2000): Hydraulics of Roman Aqueducts: Steep Chutes, Cascades, and Dropshafts. *American Journal of Archaeology*, 104, 47–72.

Culiberg, Metka (1997): Paleovegetacijske razmere v Koprskem primorju / The Paleovegetational Conditions in the Coastal Region of Koper. In: Horvat, Jana: Sermin. Prazgodovinska in zgodnjerska naselbina v severozahodni Istri / A Prehistoric and Early Roman Settlement in Northwestern Istria. Opera Instituti Archaeologici Sloveniae 3. Ljubljana, Založba ZRC, 135–138.

Degrassi, Nevio (1939): La rappresentazione dell'Istria nella Tabula Peutingeriana. *Bullettino del Museo dell'Impero romano*, 10, 65–68.

Diekamp, Anja, Stalder, Roland, Konzett, Jürgen & Peter Mirwald (2010): Lime Mortar with Natural Hydraulic Components – Characterization of Reaction Rims with FTIR-imaging in ATR-mode. In: Válek, Jan, Groot, Caspar & John J. Hughes (eds.): 2nd Conference on Historic Mortars – HMC 2010 and RILEM TC 203-RHM final workshop. Bagneux, RILEM Publications SARL, 111–118.

Drdácky, Miloš, Fratini, Fabio, Frankeová, Dita & Zuzana Slížková (2013): The Roman Mortars used in the Construction of the Ponte di Augusto (Narni, Italy) – A Comprehensive Assessment. *Construction and Building Materials*, 38, 1117–1128.

Elsen, Jan (2006): Microscopy of Historic Mortars – a Review. *Cement and Concrete Research*, 36, 8, 1416–1424.

Elsen, Jan, Van Balen, Koenraad & Gilles Mertens (2010): Hydraulicity in Historic Lime Mortars: a Review. In: Válek, Jan, Groot, Caspar & John J. Hughes (eds.): 2nd Conference on Historic Mortars – HMC 2010 and RILEM TC 203-RHM final workshop. Bagneux, RILEM Publications SARL, 129–145.

Farcas, Fabienne & Philippe Touzé (2001): La spectrométrie infrarouge à transformée de Fourier (IRTF) Une méthode intéressante pour la caractérisation des ciments. *Bulletin des laboratoires des ponts et chaussées*, 230, 77–88.

Fröhlich, Thomas (1995): Cornici di stucco di terzo e quarto stile a Pompei: alcuni dati statistici. *Mededelingen van het Nederlands Instituut te Rome*, 54, 192–199.

Guarnieri, Chiara (2016): La villa romana di Russi. Guida breve al sito archeologico. Faenza, Tipografia Faentina Editrice.

Gutman, Maja, Zanier, Katharina, Lux, Judita & Sabina Kramar (2016): Pigment Analysis of Roman Wall Paintings from Two Villas in Slovenia. *Mediterranean Archaeology & Archaeometry. International Journal*, 16, 3, 193–206.

Horgnies, Matthieu, Chen, Jeffrey J. & Catherine Bouillon (2013): Overview about the Use of Fourier Transform Infrared Spectroscopy to Study Cementitious Materials. *Materials Characterisation*, 6, 251–262.

Hughes, John J., Leslie, Alick B. & Kristof Callebaut (2001): The Petrography of Lime Inclusions in Lime Base Mortars. *Annales Geologiques des pays Helleniques, Edition Speciale*, 39, 359–364.

Hughes, Trevor L., Methven, Claire M., Jones, Timothy G. J., Pelham, Sarah E., Fletcher, Philip & Christopher Hall (1995): Determining Cement Composition by Fourier Transform Infrared Spectroscopy. *Advanced Cement Based Materials*, 2, 3, 91–104.

Indelicato, Mario (2020): Columella's Wine: a Roman Enology Experiment. *EXARC Journal*, 1. <https://exarc.net/ark:/88735/10485> (last access: 2022-01-10).

Krašna, Andrea (2022): Rimski kamniti spomeniki v zahodnem delu Slovenije. Master's thesis. Ljubljana, University of Ljubljana.

Kutnar, Matevž (2022): Rimskodobne apnenice. Bachelor's thesis. Ljubljana, University of Ljubljana.

Laycock, Elizabeth, Pirrie, Duncan, Clegg, Francis, Bell, Anthony & Paul Bidwell (2018): An Investigation to Establish the Source of the Roman Lime Mortars Used in Wallsend, UK. *Construction & Building Materials*, 196, 611–625.

Mansuelli, Guido Achille (1962): La villa romana di Russi. Faenza, Stabilimento Grafico Fratelli Lega.

Massazza, Franco (2001): Pozzolana and pozzolanic cements. In: Hewlett, Peter C. (ed.): *Lea's Chemistry of Cement and Concrete*. Oxford, Butterworth-Heinemann, 471–636.

Mehta, Pkmehta Kumar (1987): Natural Pozzolans: Supplementary Cementing Materials for Concrete. CANMET Special Publication, 86, 1–3.

Mertens, Gilles, Elsen, Jan, Brulet, Raymond, Brutsaert, Anne & Marianne Deckers (2009): Quantitative Composition of Ancient Mortars from the Notre Dame Cathedral in Tournai (Belgium). *Materials Characterization*, 60, 580–585.

Middendorf, Bernhard, Hughes, John J., Callebaut, Kristof, Baronio, Giulia & Ioanna Papayianni (2005): Investigative Methods for the Characterization of Historic Mortars – Part 2. Chemical characterization. *Materials and Structures*, 39, 771–780.

Miriello, Domenico, Barca, Donatella, Bloise, Andrea, Ciarallo, Annamaria, Crisci, Gino M., De Rose, Teresa, Gattuso, Caterina, Gazineo, Flavia & Mauro F. La Russa (2010): Characterisation of Archaeological Mortars from Pompeii (Campania, Italy) and Identification of Construction Phases by Compositional Data Analysis. *Journal of Archaeological Science*, 37, 2207–2223.

Moropoulou, Antonia, Bakolas, Asterios & Katerina Bisbikou (2000): Investigation of the Technology of Historic Mortars. *Journal of Cultural Heritage*, 1, 45–58.

Moropoulou, Antonia, Bakolas, Asterios & Eleni Aggelakopoulou (2004): Evaluation of Pozzolanic Activity of Natural and Artificial Pozzolans by Thermal Analysis. *Thermochimica Acta*, 420, 135–140.

Novšak, Matjaž & Tina Žerjal (2008): Školarice in Križišče, rimski najdišči. In: Jurković, Miljenko (ed.): *Rezultati arheoloških istraživanja na području Istre. Zbornik radova s međunarodnoga znanstvenog skupa održanog u Poreču 29. rujna 2006. Poreč, Zavičajni muzej Poreštine*, 25–34.

Novšak, Matjaž, Bekljanov Zidanšek, Iris & Tina Žerjal (2019): Križišče pri Spodnjih Škofijah. *Arheologija na avtocestah Slovenije 81*. Ljubljana, Zavod za varstvo kulturne dediščine Slovenije.

Paama, Lilli, Pitkänen, Ilkka, Rönkkömäki, Hannu & Paavo Perämäki (1998): Thermal and Infrared Spectroscopic Characterization of Historical Mortars. *Thermochimica Acta*, 320, 127–133.

Pintér, Farkas, Weber, Johannes, Bajnóczi, Bernadett & Mária Tóth (2011): Brick-Lime Mortars and Plasters of a Sixteenth Century Ottoman Bath from Budapest, Hungary. In: Turbanti-Memmi, Isabella (ed.): *Proceedings of the 37th International Symposium on Archaeometry, 12th–16th May 2008, Siena, Italy*. Berlin – Heidelberg, Springer, 293–298.

Riemenschneider, Ulrike (1986): *Pompejanische Stuckgesimse des Dritten und Vierten Stils*. Frankfurt am Main – New York, P. Lang.

Sakara Sučević, Maša, Žerjal, Tina, Gardina, Lidija & Maruša Bizjak (2015): Vsak košček šteje: Školarice: od arheološkega artefakta do muzealije / Pezzo per pezzo: Scoladizzi: musealizzazione dell'oggetto archeologico. Koper, Pokrajinski muzej Koper.

Salvadori, Monica (2012): I sistemi decorativi parietali in Cisalpina: per un inquadramento generale. In: Oriolo, Flaviana & Monika Verzár-Bass (eds.): *La pittura romana nell'Italia Settentrionale e nelle regioni limitrofe. Atti della XLI Settimana di Studi Aquileiesi, 6-8 maggio 2010*. Trieste, Editreg, 19–39.

Secco, Michele, Dilaria, Simone, Addis, Anna, Bonetto, Jacopo, Artioli, Gilberto & Monica Salvadori (2018): The Evolution of Vitruvian recipes over 500 years of floor making techniques: the case studies of the Domus Delle Bestie Ferite and the Domus di Tito Macro (Aquileia, Italy). *Archeometry*, 60, 2, 185–206.

Secco, Michele, Dilaria, Simone, Addis, Anna, Bonetto, Jacopo, Tamburini, Sergio, Preto, Nereo, Ricci, Giulia & Gilberto Artioli (2020): Technological Transfers in the Mediterranean on the Verge of Romanization: Insights from the Waterproofing Renders of Nora (Sardinia, Italy). *Journal of Cultural Heritage*, 44, 60–82.

Snellings, Ruben, Mertens, Gilles & Jan Elsen (2012): Supplementary Cementitious Materials. *Reviews in Mineralogy and Geochemistry*, 74, 211–278.

Trenz, Alfred & Matjaž Novšak (2004): *Villa rustica na lokalitetu Školarice na trasi autoputa Klanec – Ankaran*. *Histria Antiqua*, 12, 77–87.

Ventura, Paula (2001): *Villa del Randaccio*. In: Degrassi, Valentina & Aannalisa Giovannini (eds.): *Tempus edax rerum. Roma ed il Timavo. Appunti di ricerca*. Duino Aurisina, Gruppo speleologico Flondar, 36–38.

Weber, Johannes & Anthony Baragona (2021): Microscopy Brings it to Light: Roman Mortar Technology Studied by Polarizing Microscopy and SEM. In: Cavalieri, Marco & Paolo Tomassini (eds.): *La peinture murale antique: méthodes et apports d'une approche technique*. Bordeaux, Pictor collection, 229–240.

Weber, Johannes, Baragona, Anthony, Pintér, Farkas & Christophe Gosselin (2014): Hydraulicity in Ancient Mortars: Its Origin and Alteration Phenomena under the Microscope. In: Çopuroğlu, Oğuzhan (ed.): *Proceedings 15th Euroseminar on Microscopy Applied to Building Materials 16-19 June 2014*. Delft, Delft University of Technology, 1–11.

Weber, Johannes, Köberle, Thomas & Farkas Pintér (2013): Methods of Microscopy to Identify and Characterize Hydraulic Binders in Historic Mortars – a Methodological Approach. In: Hughes, John J. (ed.): *Proceedings of the 3rd Historic Mortars Conference*, 11-14 September 2013, Glasgow, 1–8.

Weber, Johannes, Prochaska, Walter & Norbert Zimmermann (2009): Microscopic Techniques to Study Roman Renders and Mural Paintings from Various Sites. *Materials Characterization*, 60, 7, 586–593.

Yu, Ping, Kirkpatrick, R. James, Poe, Brent, McMillan, Paul F. & Xiandong Cong (1999): Structure of Calcium Silicate Hydrate (C-S-H): Near, Mid and Far-infrared Spectroscopy. *Journal of the American Ceramic Society*, 82, 742–748.

Zanier, Katharina (2012): Decorazioni parietali nelle ville del Litorale sloveno: considerazioni preliminari. In: Oriolo, Flaviana & Monika Verzár-Bass (eds.): *La pittura romana nell'Italia Settentrionale e nelle regioni limitrofe*. Atti della XLI Settimana di Studi Aquileiesi, 6-8 maggio 2010. Trieste, Editreg, 459–460.

Zanier, Katharina (2020): Stenski omet in maltne podlage. In: Žerjal, Tina & Matjaž Novšak: *Školarice pri Spodnjih Škofijah*. *Arheologija na avtocestah Slovenije* 86. Ljubljana, Zavod za varstvo kulturne dediščine Slovenije, 220–234.

Žerjal, Tina & Matjaž Novšak (2020): Školarice pri Spodnjih Škofijah. *Arheologija na avtocestah Slovenije* 86. Ljubljana, Zavod za varstvo kulturne dediščine Slovenije.